이학석사학위논문

# Protein-Protein Interaction and Intercellular Movement of AT-HOOK MOTIF NUCLEAR LOCALIZED PROTEIN3 (AHL3) / AHL4 Transcriptional Factors

## AT-HOOK MOTIF NUCLEAR LOCALIZED PROTEIN 3 (AHL3) / AHL4 전사인자 사이의 상호작용과 세포 이동 연구

2016년 8월

서울대학교 대학원

생명과학부

서 민 지

# Abstract

## Protein-Protein Interaction and Intercellular Movement of AT-HOOK MOTIF NUCLEAR LOCALIZED PROTEIN3 (AHL3) / AHL4 Transcriptional Factors.

**MinJi Seo**

**School of Biological Sciences**

**The Graduate School**

**Seoul National University**

Interaction and movement of various proteins are critical steps for deciding a cell fate. Recently, two novel factors, AT-HOOK MOTIF NUCLEAR LOCALIZED PROTEIN 3 (AHL3) and AHL4 were reported to define xylem boundary in the Arabidopsis root. These two factors interact with each other and move into neighbor cells. However, which domain of these proteins are participating in the process of interaction and movement is not clear. AHL gene family member contains two conserved domains: AT-hook motif and plant and prokaryote

conserved (PPC) domain. We found that PPC domain of AHL4 protein is involved in interaction with other AHL proteins including AHL3 protein. To understand the importance of amino-acid sequence of PPC domain in the interaction, we mutated some amino-acids in PPC domain of AHL4 protein that are predicted to affect protein-protein interaction based on 3-D structure. Yeast two hybrid assay indicated that mutated AHL4 and AHL3 no longer interact each other. Furthermore, AHL3 and AHL4 interact with not only each other but also other AHLs. These protein interaction data suggest the possibility that certain amino acids of PPC domain are important for forming protein complex between AHL proteins. Moreover, swapping PPC domain between two different AHL proteins induces the change of AHL movement. Therefore, the possibility suggests that PPC domain which is related to the interaction between AHL proteins is also participated in the movement of AHL protein.

**Keywords: Protein-Protein Interaction, Intercellular Movement of Transcriptional Factors, AT-HOOK MOTIF NUCLEAR LOCALIZED PROTEIN (AHL) , plant and prokaryote conserved (PPC) domain**

**Student Number: 2014-25017**

# CONTENTS

# LIST OF FIGURES

# Ⅰ. Introduction

## Root apical meristem consists of various type of cells.

In Arabidopsis root, cell layers such as epidermis, cortex, endodermis and stele are radically organized (Figure 1). Epidermis is the most outer cell layer and it absorbs water and nutrients from soil. Some of epidermis cell differentiates into root hair cell and several transcriptional factors are involved in this process. Ground tissue consists of cortex and endodermis tissue where casprian strip is located. The differentiation process of cortex and endodermis in the ground tissue is also controlled by transcriptional factors. Stele, the most inner tissue complex surrounded by endodermis, consists of xylem, phloem and pericycle. In a transverse section of the root, xylem cells are located in central xylem axis: protoxylem cells differentiate in two marginal positions of xylem axis and metaxylem cells differentiate in the central position. The quiescent center (QC), located at the tip of root, helps to maintain the surrounding stem cells that generate radial tissues as well as root cap. Several studies showed that interaction and movement of transcription factors are important for cell type organization.

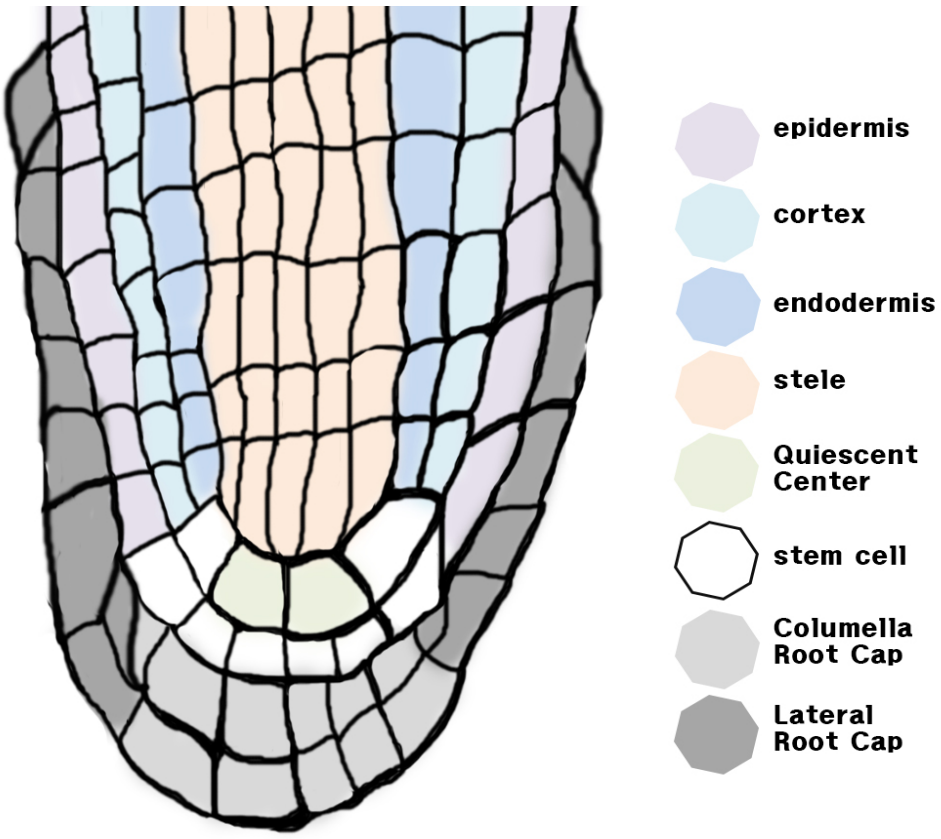


**Figure 1. Schematic representation of root apical meristem (RAM) in *Arabidopsis thaliana.***

Each representative cell types are marked in different colors.

# A mobile transcription factor in the control of root hair development.

The differentiation of root hair cell from epidermis cell is a well-known process that requires for the interaction and movement of regulatory proteins. Whether a cell becomes root hair cell or non-hair cell is determined by cell position in Arabidopsis. Root hair cell is specified on trichoblast, the epidermal cell that touches two underlying cortical cells, (Dolan et al., 1994; Dolan et al., 1993; Galway et al., 1994). Epidermal cell, which neighbors only a single cortical cell, is called atrichoblast and turned into non-hair cell (Dolan et al., 1994; Galway et al., 1994).

*GLABRA2* (*GL2*) is a gene encoding homeodomain transcription factor that promotes non-hair cell differentiation and represses hair cell differentiation (Cristina et al., 1996; Hung et al., 1998; Rerie et al., 1994). *GL2* expression is positively regulated by TRANSPARENT TESTA GLABRA1 (TTG1) protein. TTG1 encodes a WD40-repeat protein and interacts with GL3 (Bernhardt et al., 2003; Bernhardt et al., 2005; Galway et al., 1994; Walker et al., 1999). TTG-GL3 forms a protein complex together with WEREWOLF (WER) to promote GL2 expression (Lee and Schiefelbein, 1999). GL2 subsequently acts to specify the atrichoblast into non-hair cell.

In the atrichoblast, TTG-GL3 and WER protein complex also induces expression

of CAPRICE (CPC) protein (Bernhardt et al., 2003; Koshino-Kimura et al., 2005). CPC protein moves from an atrichoblast into a trichoblast and acts with a competitor of WER protein (Kurata et al., 2005; Simon et al., 2007; Tominaga-Wada et al., 2013; Wada et al., 2002). TTG1-GL3 and CPC protein complex represses expression of GL2 protein and thereby promotes hair cell differentiation (Wada et al., 2002; Wada et al., 1997).

## A mobile SHOOTROOT (SHR) controls patterning of ground tissues and vascular system

Another example of interaction and movement of proteins related to tissue patterning is the case of SHR protein and SCR protein. At first, SHR and SCR were discovered as the essential regulators of periclinal asymmetric division of cortex/endodermis initial (CEI) cell (Benfey et al., 1993; Helariutta et al., 2000; Laurenzio et al., 1996; Sabatini et al., 2003). In *shr* mutant, a single ground tissue layer expresses only cortex marker, not endodermis marker (Helariutta et al., 2000). On the other hands, in *scr* mutant, a single ground tissue layer has both endodermis and cortex characteristics (Sabatini et al., 2003). These indicate that *SHR* is important for both cell division and cell differentiation whereas *SCR* is required for the asymmetric division process. In addition, *SHR* expression does not change in *scr* mutant, however *SCR* is barely expressed in *shr* mutant (Helariutta et al., 2000; Sabatini et al., 2003). It turned out that SHR is a direct upstream-regulator of *SCR* (Cui et al., 2007).

*SHR* gene is expressed in stele (Helariutta et al., 2000). Translated SHR protein moves into neighboring cells and induces the expression of *SCR* gene in quiescent center, CEI cell and endodermis (Gallagher et al., 2004; Sabatini et al., 2003). Translated SCR protein makes a complex with moved SHR protein and this complex in the CEI induces asymmetric cell division by regulating D-type cyclin (Sozzani et al., 2010).

The protein interaction of SCR/SHR complex also contributes to xylem differentiation process (Carlsbecker et al., 2010). SHR/SCR complex in the endodermis induces microRNA165/166 transcription. MicroRNA165/166 moves into stele and targets mRNAs of HD-ZIPⅢ transcriptional factors expressed in the stele (Emery et al., 2003; Zhou et al., 2007). Resulting concentration gradient of HD-ZIPⅢ transcriptional factors decides the fate of xylem precursor cell to protoxylem when the concentration is low, or to metaxylem when the concentration is high (Carlsbecker et al., 2010).

## Two novel AT-hook family transcription factors decide xylem boundary in the root through protein-protein interaction and intercellular movement.

Procambium cells occupy adjacent to protoxylem and metaxylem cells. Xylem, the

one of main components in plant vascular system, is originated from procambium cells (Etchells and Turner, 2010; Fisher and Turner, 2007). Procambium cells have a potential to differentiate into other type cells.

Recently, *AHL3* and *AHL4* were discovered as regulators of the boundary between xylem procambium (Zhou et al., 2013). Analyses of cell type markers such as *AHP6* for identifying protoxylem precusor, *TMO5* for xylem precursor and *ARR5* for procambium indicated the expansion of protoxylem domain in *ahl4* mutant (Bishopp et al., 2011; De Rybel et al., 2013; Lee et al., 2006; Mahonen et al., 2006; Schlereth et al., 2010; Zhou et al., 2013). It was found that AHL4 can interact with AHL3, a closest one among AHL family members to form a heteromer, and has an ability to move into xylem from procambium. When *AHL4* was expressed but its intercellular movement was interfered in *ahl4* mutant background, the altered boundary between xylem and procambium could not be rescued (Zhou et al., 2013). These results suggest that interaction and intercellular movement of AHL3 and AHL4 are the important processes for deciding the boundary between xylem and procambium. Other AHL proteins, such as AHL27 and AHL29, also showed interaction with other AHL members (Street et al., 2008; Zhao et al., 2013). Taken together, shared mechanism for protein-protein interaction among AHL members might exist and this interaction might be important for molecular functions of AHLs.

## Interaction and movement of transcriptional factors are

## regulated tightly.

Generally, plasmodesmata (PD) is known as a route for intercellular movement of proteins. PD is the hole between neighbor plant cells and connects cytoplasm between two cells. The main role of PD is exchange of material and transferring signals between cells. The study with GFP protein shows that the size of PD is different according to the type or developmental stage of cells. For example, protein movement is more extensive in younger leaves than in older leaves (Oparka et al., 1999).

Two important factors affecting intercellular protein movement are known; the size of moved protein and the kinds of moved protein. Generally, bigger protein moves less actively than smaller protein. The study with single, double and triple GFP proteins visually explains the decrease of movement as GFP size increases (Crawford and Zambryski, 2000, 2001). Another important factor is type of intercellular movement. Non-targeted movement is similar to diffusion through concentration gradients (Crawford and Zambryski, 2001). GFP protein is an example of non-targeted movement. On the other hands, many kinds of mobile proteins such as signaling factors or viral proteins show that these proteins move into to certain types of neighboring cells (Matsubayashi et al., 2001). This called a targeted movement (Zambryski and Crawford, 2000). In case of targeted movement, the component of PD helps the directional movement of particular types of proteins (Zambryski and Crawford, 2000).

CPC and SHR proteins which I already mentioned move into targeted cell directly and induce the expression of other proteins. In case of CPC protein, it has a signal domain for cell-to-cell movement. N-terminal part of Myb domain in CPC protein is required for movement (Kurata et al., 2005). Amino acid substitution experiment shows that W76 and M78 amino acid residue in Myb domain is critical for targeted transport and W76 is also important to move into nucleus (Kurata et al., 2005). SHR protein also shows the targeted movement and it also has a regulatory sequence for movement. When SHR protein is expressed under SUC2 promoter, SHR protein is expressed in the phloem companion cell (CC) where SUC gene is expressed (Sena et al., 2004). However, the SHR in phloem CC cannot move into other cells. It means that phloem CC does not have some factors that help SHR to move. Amino acid substitution experiment that changes T289 to Isoleucine showed that this amino acid is important for intercellular movement of SHR (Gallagher et al., 2004).

Moreover, in two cases, the intercellular movement of proteins preceded their interaction with other proteins. When proteins make a complex, the size of complex is bigger. Therefore, the mobility of protein decreases in general. The interaction of SHR protein with SCR protein seems to function to trap SHR protein and inhibit further movement (Sena et al., 2004).

As many mobile transcriptional factors did, movement of AHL4 is important to its function. Moreover, the fact that AHL4 protein can make a complex with AHL3 protein is same as other mobile protein cases. However, which domains of AHL

proteins are participating in the protein-protein interaction and/or intercellular movement is still unknown.

## AHL proteins share common domains in its family.

To investigate more deeply in AHL4 protein, we searched for other AHL proteins which belong to same gene family. AHL proteins are known have two domain; AT-hook motif and PPC domain (Figure 2). Every AHL protein has one or two AT-hook motif and one PPC domain (Fujimoto et al., 2004; Xiao et al., 2009). AHL gene family consists of 29 proteins which are divided into Clade A and Clade B (Fujimoto et al., 2004; Zhao et al., 2013) (Figure 3). The paper of Zhao divided PPC domain into two clades according to amino acid seqeuence. Clade A has intron-less AHLs with one AT-hook motif and one PPC domain. Clade B has intron-containing AHLs with one or two AT-hook motif and one PPC domain (Zhao et al., 2013).

AT-hook motif contains a conserved palindromic core amino acid sequence (Arg-Gly-Arg) (Huth et al., 1997). These three amino acids can bind minor groove of AT-rich B form DNA (Huth et al., 1997). This AT-hook motif is found in various gene families including the high mobility group A (HMGA) proteins in mammals (Aravind and Landsman, 1998).

PPC domain is about 120 amino acids in length. In bacteria and archaea, a kind of protein which is similar to PPC domain in AHL protein exists (Lin et al., 2007; Lin

et al., 2005). The PPC proteins in prokaryotes have similar structure with one α helix and five β strands (Lin et al., 2007; Lin et al., 2005). The crystal structure of bacteria single protein implies that they form a trimer when proteins make a complex (Lin et al., 2007; Lin et al., 2005)

The research about function of AHL27 and AHL29 reports that the interaction between AHL27 and AHL29 is mediated by its PPC domain (Street et al., 2008; Zhao et al., 2013). However, the core six amino acids (Gly-Arg-Phe-Glu-Ile-Leu) in PPC domain do not affect the interaction between AHL proteins (Zhao et al., 2013). The six amino acids seem to affect the interaction with non-AHL proteins such as transcriptional factor TCP4 (Zhao et al., 2013).

In this thesis, we investigated that the interaction of AHL3 with other AHL protein members. AHL3 protein can interact with not only AHL4 but also other AHL proteins, which are expressed in root stele. AHL4 also interacts with other AHLs. These suggest the AHL3/4 complex might make larger protein complex with other AHL protein together. Next, we tried to find which domain is involved in the protein-protein interaction. The interaction between AHL3 and AHL4 is also mediated by its PPC domain, like AHL27 and AHL 29. To find which amino-acid in PPC domain is important to interact, modified AHL4 protein with three amino-acid mutations was made. Mutated AHL4 did not show interaction with AHL3 protein. Therefore, the mutated amino-acids are important for interaction. We also asked whether the PPC domain sequence is important for intercellular movement. In previous data, we showed that AHL4 protein expressed in the stele moves into

endodermis cell, whereas AHL1 protein cannot. The AHL4 protein whose PPC domain was swapped with PPC domain of AHL5 protein spread more broadly than non-modified AHL4 protein. It means PPC domain sequence of AHL4 is important to move. Collectively, this thesis shows the importance of protein-protein interaction in the intercellular trafficking of AHL3/4. Further studies will lead us to understand how intercellular movement of AHl3/4 modulates xylem boundary in Arabidopsis root.

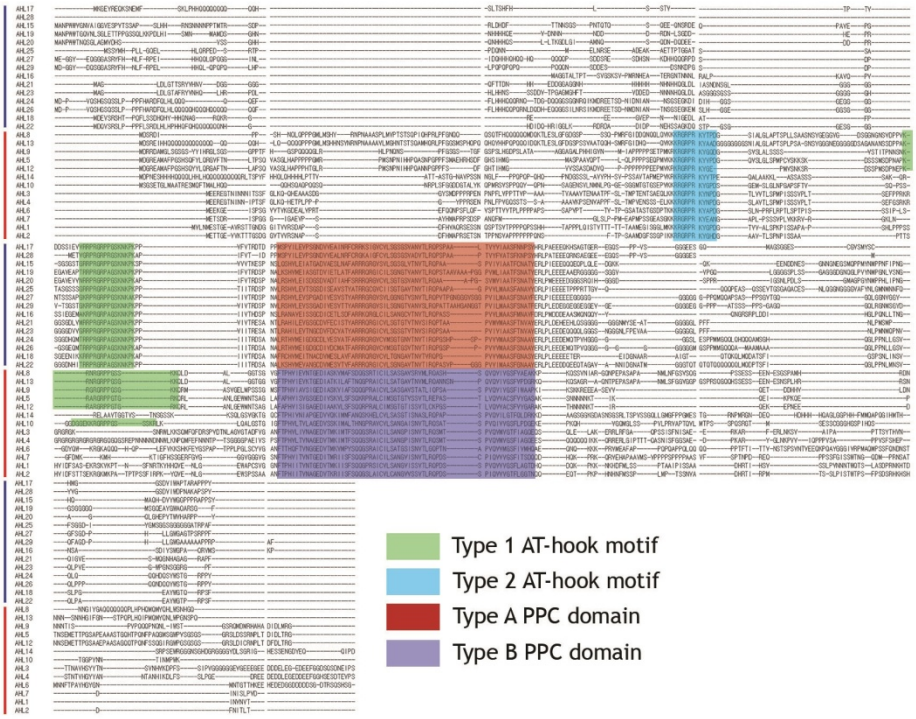


**Figure 2. Protein sequence alignment of AHL protein family.**

**All the AHL proteins have two kinds of domain, AT-hook motif and PPC domain. Typical domains in proteins indicate by color box. AHL3 and AHL4 have one Type 2 AT-hook motif and one Type B PPC domain.**

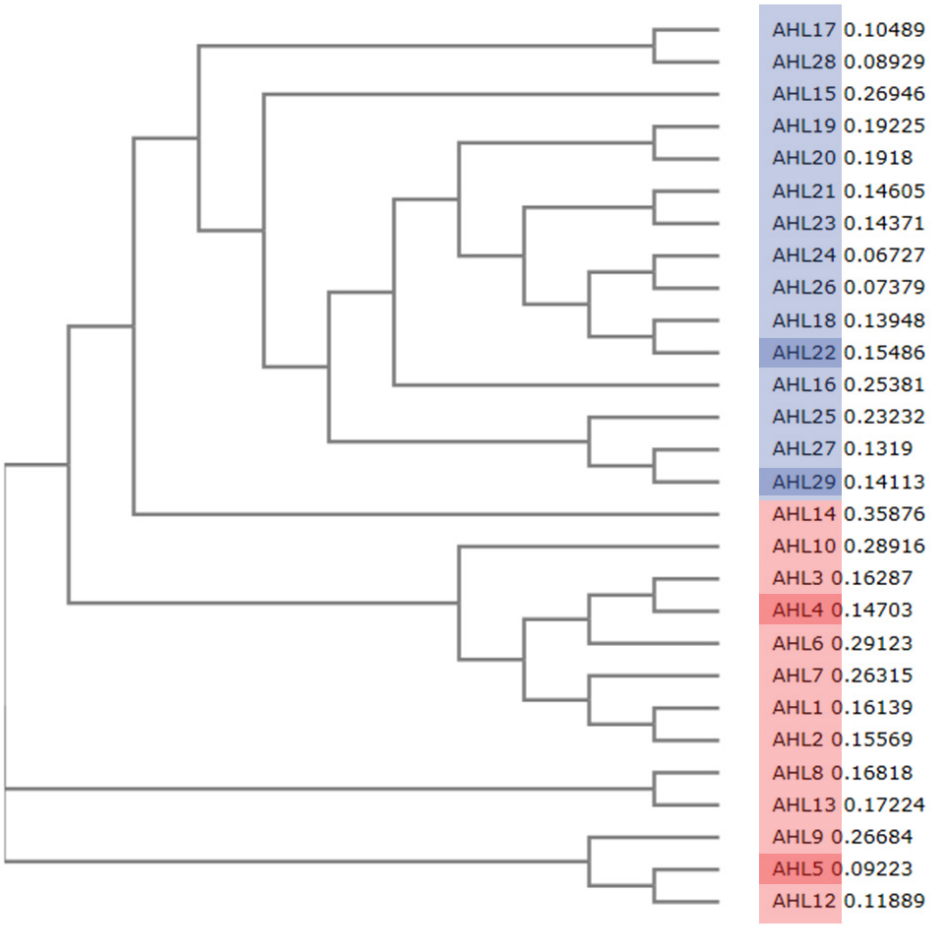


**Figure 3. Phylogenetic tree of AHL gene family.**

AHL gene family consists of 29 AHL genes. 29 AHL genes divide into 2 clades, Clade A and Clade B. *AHL3* and *AHL4*, which are related to deciding to xylem boundary, belong to clade B. Marked AHL proteins (AHL22, AHL29, AHL4, AHL5) indicate their predicted 3D structure in Figure

# Ⅱ. Materials & Methods

## Plant materials and growth conditions

*Arabidopsis thaliana* ecotype Col-0 was used in this research. *ahl4-1* (SALK_124619) seed was obtained from the ABRC (Zhou et al., 2013). AHL4::GUS and AHL4::AHL4:GFP transgenic plants were generated by Dr. Jing Zhou, a former lab member (Zhou et al., 2013).

Seedlings for root analysis were germinated and grown on Murashige and Skoog (MS) medium. MS medium contained 4.33 g of Murashige and Skoog Basal salts, 0.5 g of MES hydrate and 10 g of sucrose per one liter. pH of MS media was adjusted to 5.7 ~ 5.8 with 5 M potassium hydroxide solution. Media were autoclaved at 121 ˚C for 20 minutes. Some seedlings were transplanted onto the soil and then grown in the growth room, which is maintained at 22 ˚C with a cycle of 16 hour day and 8 hour night.

## AHL gene cloning

All the AHL gene coding regions were amplified from cDNA of Col-0 using polymerase chain reaction (PCR). PCR reactions were performed using Phusion®

High-Fidelity DNA Polymerase (NEW ENGLAND BioLabs). Forward primers and reverse primers used in PCRs are indicated in Table 1. PCRs were operated with 37 cycles of 30 seconds of denaturation at 98 ˚C, 30 seconds of annealing at 60 ˚C, and 1 minute 30 seconds of elongation time at 72 ˚C. Amplified DNAs from PCR were purified by HiGene™ Gel and PCR purification system (BIOFACT) and inserted into pENTR/D-TOPO vector by TOPO™ Cloning reaction. For TOPO reaction, 2ul of fresh PCR products, 0.5ul of Salt solution and 0.5ul of TOPO vector were mixed and incubated 5min at room temperature. Then, TOPO reaction mixture was transformed into *E.coli* and transformed colonies were selected on Luria-Bertani (LB) agar media supplemented with kanamycin (50 μg/ml) antibiotic. The selected colonies were inoculated to obtain cloned pENTR vectors by mini-prep.

## Site-directed mutagenesis

For substituting selected amino acids, we performed PCR based site-directed mutagenesis. Our primer sets for site-directed mutagenesis were listed in Table 2.
The reaction product contained 5 μl of 10× reaction buffer, 2 μl of AHL4 in pDONR221 vector (10 ng/μl), 1μl of forward primer F1 (10 pmol/μl), 1 μl of reverse primer R1 (10 pmol/μl), 2 μl of dNTP mixture (each 2.5 mM), 38 μl of dH2O and 1μl Muta-direct™ Enzyme. Then, PCRs were operated with Pre-denaturation step at 95 ˚C for 30 seconds and 15 cycles of 98 ˚C for 30

seconds of, 55 ˚C for 1 minutes and 72 ˚C for 3 minutes.

After finishing site-mutagenesis reaction , we put the PCR product into ice for 5 minutes and stored at room temperature. Then, we added 1 μl (10 U/μl) of Mutazyme™ Enzyme into the mixture and incubated at 37 ˚C for 1 hour. Next, we put the 10 μl of product into 50 ul of DH5a (dam+ strain) competent cell to proceed heat-shock transformation.

**Table 1. Primer sets for AHL genes cloning.**

| Name | Sequence |
|---|---|
| **AHL2_F** | 5'-CAC CAT GGA GAC TAC CGG AGA AGT TG-3' (26mer) |
| **AHL2_R_NS** | 5'-CGT CAA AGT GAT ATT AAA GTC ATG A-3' (25mer) |
| **AHL5_F** | 5'-CAC CAT GGA TGG GAG AGA AGC TAT -3' (24mer) |
| **AHL5_R_NS** | 5'-CCC GCG AGT CAA GTC AAT ATC A-3' (22mer) |
| **AHL6_F** | 5'-CAC CAT GGA GGA GAA AGG TGA AAT-3' (24mer) |
| **AHL6_R_NS** | 5'-ACC ACT ATG AGA TTG GCT CCT A-3' (22mer) |
| **AHL7_F** | 5'-CAC CAT GGA AAC AAG CGA CAG AAT–3' (24mer) |
| **AHL7_R_NS** | 5'-GTC GAC TGG TAA AGA TAT GTT G-3' (22mer) |
| **AHL8_F** | 5'-CAC CAT GGA TTC CAG AGA CAT CCC AC-3' (26mer) |
| **AHL8_R_NS** | 5'-TTG ACC ATG ATT AGA CCA AAG ATG T-3' (25mer) |
| **AHL10_F** | 5'-CAC CAT GTC AGG ATC TGA GAC GGG–3' (24mer) |
| **AHL10_R_NS** | 5'-CTT CCA GGG CAT GTT AAT GGT G-3' (22mer) |
| **AHL12_F** | 5'–CAC CAT GGA CGG AAG AGA AGC AAT-3' (24mer) |
| **AHL12_R_NS** | 5'-TCC ACG AGT CAA ATC AAA ATC A-3' (22mer) |
| **AHL13_F** | 5'-CAC CAT GGA TTC CAG AGA GAT CCA-3' (24mer) |
| **AHL13_R_NS** | 5'-TTG AGG ACT GTT GCC AGG CCA G-3' (22mer) |
| **AHL15_F** | 5'-CAC CAT GGC GAA TCC TTG GTG GGT A-3' (25mer) |
| **AHL15_R_NS** | 5'-ATA CGA AGG AGG AGC ACG AGG C-3' (22mer) |
| **AHL16_F** | 5'-CAC CAT GGC TGG AGG TAC AGC TCT AA-3' (26mer) |
| **AHL16_R_NS** | 5'-AGG TTT CGA CAT GAC ACG CTG C-3' (22mer) |
| **AHL17_F** | 5'-CAC CAT GAA AGG TGA ATA CAG AGA GC-3' (26mer) |

| | |
|---|---|
| **AHL17_R_NS** | 5'-GTA TGG CGG TGG AGC TCT GGC-3' (21mer) |
| **AHL19_F** | 5'-CAC CAT GGC GAA TCC ATG GTG GAC AG-3' (26mer) |
| **AHL19_R_NS** | 5'-AAA TCC TGA CCT AGC TTG AGC CCA A-3' (25mer) |
| **AHL20_F** | 5'-CAC CAT GGC AAA CCC TTG GTG GAC GA-3' (26mer) |
| **AHL20_R_NS** | 5'-GTA AGG TGG TCT TGC GTG GAC-3' (21mer) |
| **AHL21_F** | 5'-CAC CAT GGC TGG TCT CGA TCT AGG CA-3' (26mer) |
| **AHL21_R_NS** | 5'-AAA CGG AGC CCT ACC GGC GC-3' (20mer) |
| **AHL22_F** | 5'-CAC CAT GGA TCA GGT CTC TCG CTC TC-3' (26mer) |
| **AHL22_R_NS** | 5'-GAA AGA TGG TCT CGG AGT TCC C-3' (22mer) |
| **AHL23_F** | 5'-CAC CAT GGC TGG TCT TGA TCT AGG CA-3' (26mer) |
| **AHL23_R_NS** | 5'-GAA AGG ACC TCT TCC ACC GGA A-3' (22mer) |
| **AHL27_F** | 5'-CAC CAT GGA AGG CGG TTA CGA GCA A-3' (25mer) |
| **AHL27_R_NS** | 5'-AAA AGG TGG TCT TGA AGG TGT TCC A-3' (25mer) |
| **AHL29_F** | 5'-CAC CAT GGA CGG TGG TTA CGA TCA ATC-3' (27mer) |
| **AHL29_R_NS** | 5'-AAA GGC TGG TCT TGG TGG TGC G-3' (22mer) |

**Table 2. Primers used for site-directed mutagenesis.**

| Name | Sequence |
|---|---|
| **Primer 1_F** | 5'- tcg cgt gct att tgt gct ctt tca gcg aac -3' Tm 79.5 |
| **Primer 1_R** | 5'- gtt cgc tga aag agc aca aat agc acg cga-3' |
| **Primer 2_F** | 5'- ggt ccc ata tcc gct gtt aca ctt cgt caa tct -3' Tm 80.924 |
| **Primer2_R** | 5'- aga ttg acg aag tgt aac agc gga tat ggg acc-3 |
| **Primer3_F** | 5'- c act tat gag ggt cat ttt gcg att ctt tct ttg acg -3' Tm 79.87 |
| **Primer3_R** | 5'-cgt caa aga aag aat cgc aaa atg acc ctc ata agt g-3' |

.

**Table 3. primers for swapping PPC domain**

| Name | Sequence |
|---|---|
| **AHL5_PPC_Not Ⅰ_F** | 5’-gcg gcc gcc ggt gag tgg atg aat aca tca gct -3’ |
| **AHL5_PPC_Sma Ⅰ_R** | 5’- gtt cgc tga aag agc aca aat agc acg cga-3’ |
| **AHL4_PPC_Sma Ⅰ_F** | 5’-/5phos/ atc aat caa tcc cgg gca aga tgg tcg tgt ctt tgg tgg tgg -3’ |
| **AHL4_-PPC_Not Ⅰ_R** | 5’-/5phos/ gcg gcc gcc aga agt agg agt gtt gttgtt aaa -3’ |

## Replacing PPC domain of AHL4 with the PPC domain of AHL5

To generate recombinant AHL4 whose PPC domain was replaced with PPC domain of AHL5, first, we designed PPC domain of AHL5 by primers anchored with Not Ⅰ recognition site at forward primer and Sma Ⅰ recognition site at reverse primer. PCRs for amplifying PPC domain of AHL5 were operated with 37 cycles of 30 seconds of denaturation at 98 ˚C, 30 seconds of annealing at 60 ˚C, and 30 seconds of elongation time at 72 ˚C. We also designed primers for pDONR221 vector with wild-type *AHL4* gene excluding PPC domain (AHL4-PPC). Primers for AHL4-PPC included Not Ⅰ recognition site at forward primer and Sma Ⅰ recognition site at reverse primer. PCRs for amplifying pDONR221 vector with AHL4-PPC were operated with 37 cycles of 30 seconds of denaturation at 98 ˚C, 30 seconds of annealing at 60 ˚C, and 30 seconds of elongation time at 72 ˚C. Primer sequences are indicated in Table 3.

Then, we treated PCR amplicants with restriction enzymes, Not Ⅰ and Sma Ⅰ in appropriated conditions, and ligated two DNA fragments using T4 DNA Ligase. After transforming the ligation mixture into *E.coli* and confirming the sequence of cloned DNA products, we performed LR reaction by mixing AHL4 promoter in

pDONR P4-P1R, AHL4 with substituted AHL5 PPC domain in pDONR221, cGFP in pDONR P2R-L3, and dpGreen BarT vector with Invitrogen™ Gateway™ LR Clonase™ II plus enzyme mix.

## LR reaction

For checking gene expression in plant, we inserted each AHL genes to pDONR221 vector. LR cloning was performed to generate AHL fused to GFP driven under WOODENLEG (WOL) promoter, a stele specific promoter in the root (Mahonen et al., 2006). 1 μl of 5 pmole each entry vectors containing each construct (pWOL, AHL gene and nos-cGFP) and 1 μl of 10 pmole dpGreen-BarT vector were mixed. The dpGreenBarT was used as a destination vector (Carlsbecker et al., 2010). Then, 1 μl of LR Clonase™ Two Plus was added, mixed well, and incubated in a thermocycler set at 25 °C overnight. Next day, we added protease K into reaction mixture and incubated at 37 °C for 10 minutes. After then, the mixture was transformed into *E.coli* competent cell using heat-shock method. Recombinant colonies were selected on LB agar media supplemented with spectromycin (100 μg/ml). Recombinants were further examined by growing *E.coli* from each colony and harvesting plasmid DNA using iNtRON Biotechnology DNA-spin™ Plasmid DNA Purification Kit.

For doing yeast-two hybrid reaction, we inserted each AHL genes in entry clone, pDONR221 vector. Cloned AHL genes were inserted into pDEST22 destination

vector and pDEST32 destination vector by GATEWAY® LR cloning technology (Invitrogen). First, 0.5 μl of each entry vectors (150nmole/ μl), 0.5 μl of pDEST22 vector (150nmole/ μl) or pDEST32 vector (150nmole/ μl) and 3 μl Tris-EDTA buffer (pH 8.0) were mixed. Then, 1 μl of LR Clonase™ Two was mixed and incubate at 25 ˚C for 1 hour. After then, the mixture was transformed into *E.coli* competent cell using heat-shock method. Recombinant colonies were selected on LB agar media supplemented with carbenicillin (50 μg/mol) or gentamycin (30 μg/ml). Recombinants were further examined by growing *E.coli* from each colony and harvesting plasmid DNA using iNtRON Biotechnology DNA-spin™ Plasmid DNA Purification Kit.

## Yeast-two-hybrid assay

To prepare for competent yeast cells, we inoculated a colony of yeast strain MaV203 into 5 ml of YPD (10g/L yeast extract, 20g/L peptone, 20g/L dextrose) and cultured overnight at 30 ˚C. And then the primary culture was added to 300ml YPD medium at 30 ˚C for 3 hours with shaking until OD600 reached to 0.5. Then, cultured yeast cells were transferred into 250 ml sterile centrifuge tubes and harvested by precipitating them at 2600 rpm for 5 minutes at room temperature. After then, the supernatant was discarded and the cell pellets were re-suspended in 50 ml of 1X TE buffer (10mM Tris-HCL (pH7.5) and 1mM EDTA). Suspended cells were centrifuged again at 2600 rpm for 5 minutes at room temperature. The

cell pellet was re-suspended in 1.5 ml of prepared, sterile 1 X TE /1X LiAC buffer. 1X LiAC buffer contained 1M LiAC solution. Then, 1 µl of prepared each plasmid DNA (100ng/ul) , 0.1 mg of herring tested carrier DNA (Invitrogen), 100 µl of competent cells and 600 µl of 50% PEG / 1X TE / 1X LiAC buffer solution were added into 1.5 ml tube. The mixture was incubated at 30 °C for 30 minutes with shaking. After then, 70 µl of DMSO (Dimethyl Sulfoxide) was added into mixture and heat-shocked for 15 minutes in 42 °C water bath. Then, cells were chilled on ice for 2 minutes. After then, cells were centrifuged at 13000 rpm for 5 seconds and supernatant was discarded. Then, cell pellet, re-suspended in 100 µl of 1X TE buffer, plated on $SD^{-Leu}$ or $SD^{-Trp}$ medium for cloned in pDEST22 or pDEST32 vectors, respectively.

Plasmid between pDEST32 and pDEST22 vector were used as negative control and pEXP32-Krev1 and pEXP22-RalGDS-wt were used as strong positive control. First, we dropped each transformants on $SD^{2-(Leu/Trp)}$ media for assay and cultured for 2days at 30 °C. Then, we put Whatman #5 filter paper over colonies by using focep and gently rubbed. When filter paper has been wetted, we carefully lifted filter paper off the $SD^{2-(Leu/Trp)}$ medium with forceps and transferred the filter paper into liquid nitrogen. After then, the filter paper soaked into X-gal assay solution (1 ml of Z buffer, 2.7 µl of $\beta$-mercaptoethanol and 16.7 µl of X-gal stock solution). Z buffer contained $Na_2HPO_4 \cdot 7H_2O$ (16.1 g/L), $NaH_2PO_4 \cdot H_2O$ (5.50 g/L), KCl (0.75 g/L), and $MgSO_4 \cdot 7H_2O$ (0.246 g/L) and adjusted to pH 7.0. X-gal stock

solution was made by dissolving 5-bromo-4-chloro-3-indolyl-b-D-galactopyranoside (X-GAL) in DMSO at a concentration of 20 mg/ml. Then, filter paper was incubated at 30 ˚C for 2 hours and we checked for the appearance of blue colonies.

## Plant transformation using floral dipping

To introduce the constructs into the Arabidopsis genome, the constructs were first transformed into *Agrobacterium tumefaciens*. First, constructed binary vector was transformed into *Agrobacterium* strain GV3101 with pSOUP by electroporation using Micro-Pulser™ (BIORAD) pursing 2.2 kv for 5 mS. Electroporated *Agrobacterium* was mixed in Super Optimal broth with Catabolite repression (S.O.C) solution, incubated at 28 ˚C for 3 hour, and plated on LB agar media supplemented with spectromycin (100 μg/ml) and gentamacyin (30 μg/ml). Selected *Agrobacterium* colony was inoculated and cultured in 5ml of LB with spectromycin (100 μg/ml) and gentamycin (30 μg/ml) for two days at 30 ˚C with shaking. Then, 1 ml of cultured *Agrobacterium* was inoculated into 100 ml of LB supplemented with spectromycin (100 μg/ml) and gentamycin (30 μg/ml) and incubated for 16-20 hours at 30 ˚C in the shaking incubator.

On the day of plant transformation, 100 ml of infiltration media was prepared for 100 ml of cultured *Agrobacterium* (Clough and Bent, 1998). 100 ml of infiltration

media contains 5 g of sucrose, 0.175 g of $MgCl_2 \cdot 7H_2O$ and 20.4 μl of Silwet. Incubated *Agrobacterium* was harvested by centrifuging at 4800 rpm for 12 minutes in 25 ˚C (HANIL Supra 22k, with S150T-4 rotor). After removing supernatant, the cell pellet was re-suspended with infiltration media. Inflorescences of prepared plants were dipped into the media (Clough and Bent, 1998). After dipping, plants were laid on a tray and were left in dark state for a day. Then, plants were placed upright and grown until their seeds were mature enough to be harvested.

## Confocal microscopy

To visualize GFP protein, 5 DAT (Day after transfer) of seedling were stained with 10 μg/ml PI (Propidium Iodide) solution (Life technologies) for 2 minutes and imaged with confocal microscope. 500x PI solution (5 mg/ml) was prepared and diluted in water before staining. The images were taken on Carl Zeiss LSM700 confocal microscope with argon ion laser (488 nm excitation, 509 nm emission for GFP, 493 nm excitation, 636 nm emission for PI).

## GUS staining

We used 5 DAT seedlings for GUS staining. First, we made GUS stock buffer containing 5 ml of 1M $NaPO_4$ buffer (pH 7.0), 5 ml of 50 mM $K_3Fe(CN)_6$, 5 ml of 50 mM $K_4Fe(CN)_6$, 5 ml of 10% Triton (50ml) , 100 μl of 0.5M EDTA and 29.9

ml of $H_2O$. The solution kept in dark. We poured 5ml of Gus stock solution into 6-wells plate and added 200 μl of 25 mg/ml X-gluc solution. We put seedlings into the solution. After we treated GUS staining solution, the sample was incubated at 37 ˚C for overnight in the dark. Next day, we cleared samples by ethanol series.

# Ⅲ. Results

## Search for AHL members that potentially interact with AHL3/4 in the root apical meristem.

To investigate the interaction of AHL3 (AT4G25320) and AHL4 (AT5G51590), we searched other AHL proteins which included into same gene family. According to the previous research in our lab, *AHL4* is expressed in the procambium of the root meristem (Zhou et al., 2013). *AHL3* is expressed in elongation and maturation zone, however, AHL3 protein is found in stele of the root meristem (Zhou et al., 2013). Therefore, we considered any AHL member expressed in the root stele as a candidate that interacts with AHL3/4 protein.

AHL family consists of 29 genes in *Arabidopsis thaliana*. Based on cell type specific root expression data (Brady et al., 2007), we selected 19 genes, expressed in the root stele where AHL4 and AHL3 protein function, as candidates. First, we checked the absolute expression level of each AHL genes in the root stele using eFP browser (http://bar.utoronto.ca/efp/cgi-bin/efpWeb.cgi?dataSource=Root). The arranged expression data are shown in Figure 4. A gene with expression value below 20.0 was excluded from candidates. For *AHL18, AHL24, AHL25* and *AHL26*, there were no gene expression data available. The genes that are expressed in the stele under our criterion are *AHL1* (*AT4G12080*), *AHL2 (AT4G22770), AHL3,*

*AHL4, AHL5 (AT1G63470), AHL6 (AT5G62260), AHL7 (AT4G00200), AHL10 (AT2G33620), AHL12 (AT1G63480), AHL13 (AT4G17950), AHL14 (AT3G04590), AHL15 (AT3G55560), AHL19 (AT3G04570), AHL20 (AT4G14465), AHL21 (AT2G35270), AHL22 (AT2G45430), AHL23 (AT4G17800), AHL27 (AT1G20900) and AHL29 (AT1G76500)*. We also included *AHL8 (AT5G46640), AHL16 (AT2G42940) and AHL17 (AT5G49700)* that are expressed at a very low level in the root stele as potential negative control.

Next, selected AHL genes were cloned into pENTR/SD/D-TOPO vectors to analyze their interaction with AHL3 and AHL4. Using cDNA prepared from 7 day old seedlings' total RNA as template, Polymerase Chain Reaction (PCR) was performed to amplify coding sequence (CDS) region of each AHL genes. Because *AHL1, AHL3, AHL4, AHL6, AHL7, AHL10, AHL12,* and *AHL13* were already cloned into pENTR/SD/D-TOPO vector by Dr. Kookhui Ryu, the former postdoc in our group, we cloned remaining AHL genes. For directional cloning, CACC was attached right before ATG, the start codon of each AHL gene, when the forward primers were designed. Stop codons were excluded in reverse primers so that cloned AHL can be translationally fused to GFP or other tags in follow-up experiments. AHL PCR amplicants were extracted from agarose gel and then inserted into pENTR/SD/D-TOPO vector by using Invitrogen™ TOPO™ PCR Cloning.

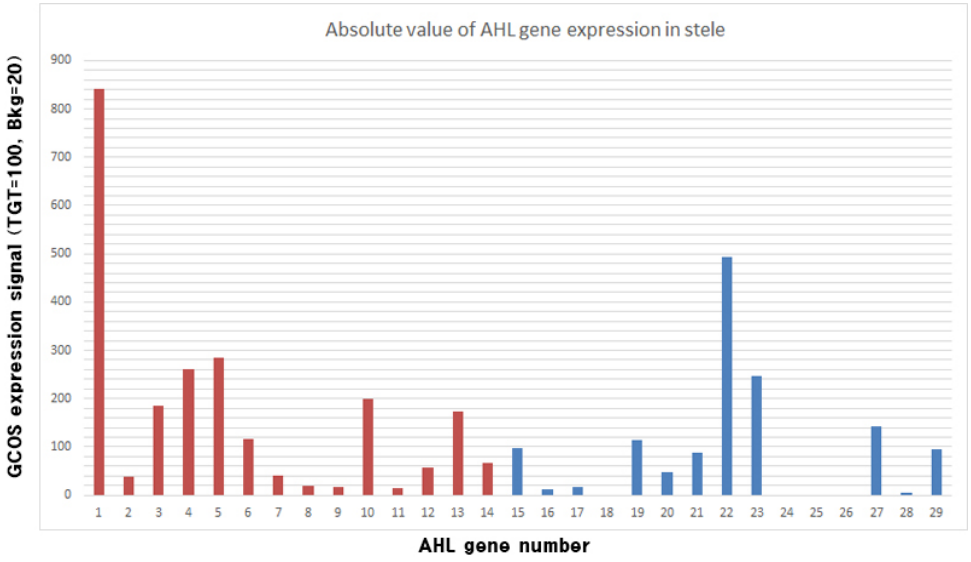


**Figure 4. Absolute expression levels of AHL genes in the root stele.**

Using eFP web site, we gained the absolute value of AHL gene expression in stele. AHLs in clade B are marked in red color and AHLs in clade A are in blue color in the graph. AHLs with expression values below 20.0 were excluded from candidates. *AHL18, AHL24, AHL25* and *AHL26* have no expression data available.

## AHL3 and AHL4 interact with multiple members of AT-hook family transcription factors.

Yeast-2-hybrid assay to find interactions between AHL3 and other AHLs was performed using ProQuest™ Two-Hybrid System with Gateway® Technology. After confirming sequences of AHL genes in pENTR/SD/D-TOPO vector, we inserted these into yeast expression vectors, pDEST22 and pDEST32 by Invitrogen™ Gateway™ LR Clonase™ II enzyme mix. In the previous study AHL4 showed auto-activation in yeast-2-hybrid assay when it was used as a bait (Zhou et al., 2013). AHL3 protein, which is 69 % identical to AHL4 in amino acid sequences, did not show auto-activation (Zhou et al., 2013). Therefore, the primary yeast-2-hybrid assay was performed using AHL3 as a bait.

X-gal assay using AHL3 and candidate AHL proteins is shown in Figure 5. As a negative control, yeast with pDEST22 vector and pDEST32 vector without inserts was used. In this case, yeast only expresses DNA-Binding domain (DBD) and activating domain (AD) domain of GAL4, without mediating interactors. As positive control, Gras protein with DBD and Krev protein with AD were used. Gras and Krev proteins were already well-known as strong interactors (Morohashi et al., 2003; Serebriiskii et al., 1999). I also checked auto-activation of AHL3 protein and confirmed that AHL3 does not show auto-activation (Figure 5A). Then, we checked the interaction between AHL3 with DBD and AHL proteins with AD. AHL1, AHL4, AHL5, AHL6, AHL7, AHL10, AHL12 and AHL13 protein with

AD showed blue color. It means that they interact with AHL3 protein.

We also checked the interaction between AHL proteins with DBD and AHL3 with AD. Auto-activation assay of each AHL proteins is shown in Figure 5B. AHL1, AHL7 showed very weak auto-activation and AHL13 showed strong auto-activation. Comparing the results from the interaction assay between AHL proteins with DBD and AHL3 with AD and the auto-activation assay result (Figure 5B, 5C) suggests that AHL1, AHL2, AHL6, AHL7 AHL10, AHL12, and AHL15 can interact with AHL3 protein.

Taking interaction data of AHL3 together, we conclude that AHL3 can interact with multiple members of AT-hook family transcription factors that belong to clade B. These are AHL1, AHL2, AHL4, AHL5, AHL6, AHL7, AHL10, and AHL12. In addition, we found that AHL3 can interact with few members in the clade A such as AHL13 and AHL15

Because AHL4 protein has auto-activation (Zhou et al., 2013), we did only X-gal assay using other AHL proteins as baits. Considering into auto-activation, AHL1, AHL3, AHL5, AHL6, AHL7, AHL10, AHL15 can interact with AHL4 proteins. (Figure 6). AHL1, AHL3, AHL5, AHL6, AHL7, AHL10 belongs to clade B. AHL15 belongs to clade A.

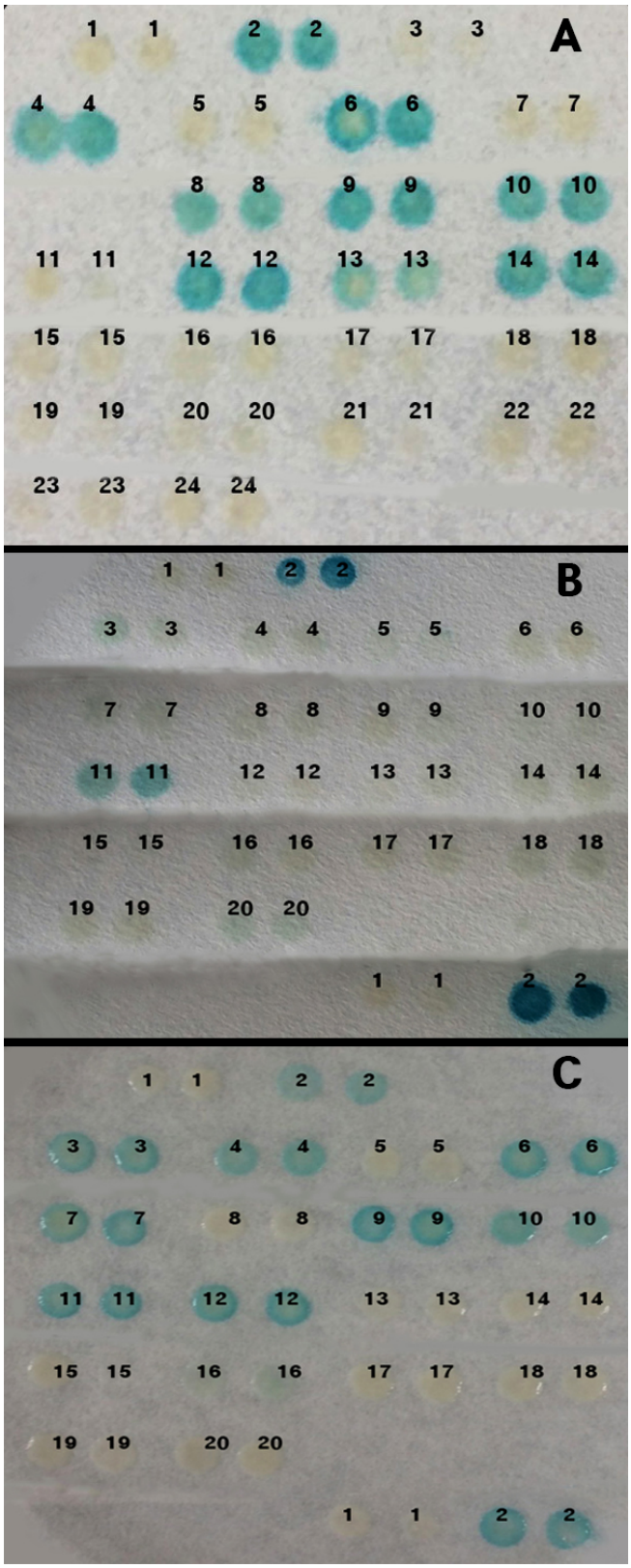
A
1 1 2 2 3 3
4 4 5 5 6 6 7 7
8 8 9 9 10 10
11 11 12 12 13 13 14 14
15 15 16 16 17 17 18 18
19 19 20 20 21 21 22 22
23 23 24 24
B
1 1 2 2
3 3 4 4 5 5 6 6
7 7 8 8 9 9 10 10
11 11 12 12 13 13 14 14
15 15 16 16 17 17 18 18
19 19 20 20
1 1 2 2
C
1 1 2 2
3 3 4 4 5 5 6 6
7 7 8 8 9 9 10 10
11 11 12 12 13 13 14 14
15 15 16 16 17 17 18 18
19 19 20 20
1 1 2 2

**Figure 5. Yeast-2-hybrid assay between AHL3 and other AHLs.**

**A)** Result of X-gal assay for checking between AHL3 and other AHL

[1 : DBD / AD , 2: DBD-GRAS / AD-Krev , 3: DBD-AHL3 / AD ,

4: DBD-AHL3 / AD-AHL1, 5: DBD- AHL3 / AD-AHL2,

6: DBD-AHL3 / AD-AHL4, 7: DBD-AHL3 / AD-AHL4*,

8: DBD -AHL3/ AD-AHL5, 9: DBD-AHL3 / AD-AHL6,

10: DBD-AHL3 / AD-AH7, 11: DBD-AHL3 / AD-AHL8,

12: DBD-AHL3 / AD-AHL10, 13: DBD-AHL3 / AD-AHL12,

14: DBD-AHL3 / AD-AHL13, 15: DBD-AHL3 / AD-AHL15,

16: DBD-AHL3 / AD-AHL16, 17: DBD-AHL3 / AD-AHL17,

18: DBD-AHL3 / AD-AHL19, 19: DBD-AHL3 / AD-AHL20,

20: DBD-AHL3 / AD-AHL21, 21: DBD-AHL3 / AD-AHL22,

22: DBD-AHL3 / AD-AHL23, 23: DBD-AHL3 / AD-AHL27,

24: DBD-AHL3 / AD-AHL29]

**B)** Result of X-gal assay for checking auto-activation of AHL proteins

[1 : DBD / AD, 2: DBD-GRAS / AD-Krev, 3: DBD-AHL1 / AD,

4: DBD-AHL2 / AD, 5: DBD-AHL5 / AD, 6: DBD-AHL6 / AD,

7: DBD-AHL7 / AD, 8: DBD-AHL8 / AD, 9: DBD-AHL10 / AD,

10: DBD-AHL12 / AD, 11: DBD-AHL13 / AD,

12: DBD-AHL15 / AD, 13: DBD-AHL16 / AD,

14: DBD-AHL19 / AD, 15: DBD-AHL20 / AD,

16: DBD-AHL21 / AD, 17: DBD-AHL22 / AD,

18: DBD-AHL23 / AD, 19: DBD-AHL27 / AD,

20: DBD-AHL29 / AD ]

**C)** Result of X-gal assay for checking between AHL proteins and AHL3

[1 : DBD / AD, 2: DBD-GRAS / AD-Krev,

3: DBD-AHL1 / AD-AHL3, 4: DBD-AHL2 / AD-AHL3,

5: DBD-AHL5 / AD-AHL3, 6: DBD-AHL6 / AD-AHL3,

7: DBD-AHL7 / AD-AHL3, 8: DBD-AHL8 / AD-AHL3,

9: DBD-AHL10 / AD-AHL3, 10: DBD-AHL12 / AD-AHL3,

11: DBD-AHL13 / AD-AHL3, 12: DBD-AHL15 / AD-AHL3,

13: DBD-AHL16 / AD-AHL3, 14: DBD-AHL19 / AD-AHL3,

15: DBD-AHL20 / AD-AHL3, 16: DBD-AHL21 / AD-AHL3,

17: DBD-AHL22 / AD-AHL3, 18: DBD-AHL23 / AD-AHL3,

19: DBD-AHL27 / AD-AHL3, 20: DBD-AHL29 / AD-AHL3 ]

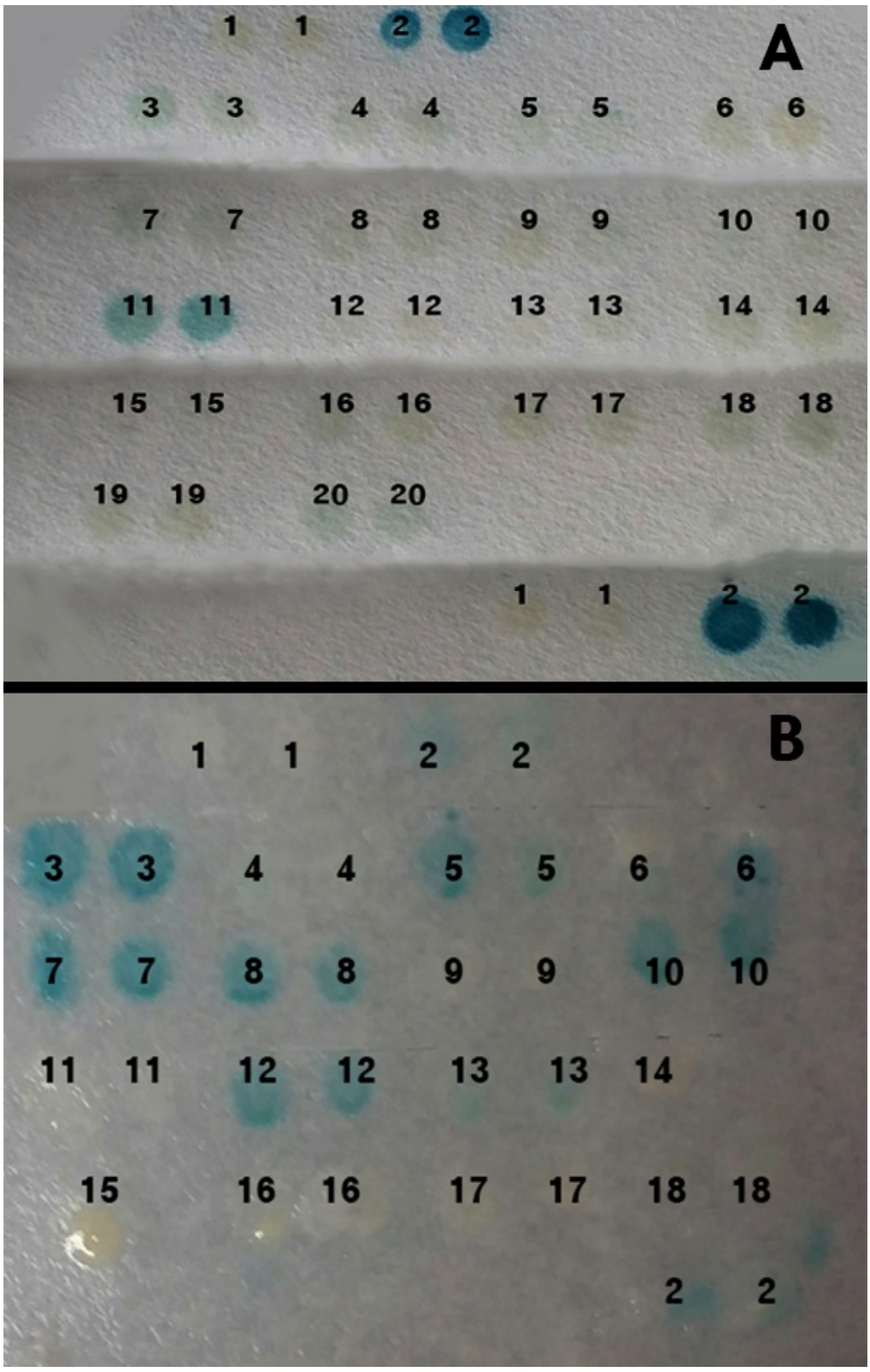
A
1 1 2 2
3 3 4 4 5 5 6 6
7 7 8 8 9 9 10 10
11 11 12 12 13 13 14 14
15 15 16 16 17 17 18 18
19 19 20 20
1 1 2 2
B
1 1 2 2
3 3 4 4 5 5 6 6
7 7 8 8 9 9 10 10
11 11 12 12 13 13 14
15 16 16 17 17 18 18
2 2

**Figure 6. Yeast-2-hybrid assay between AHL4 and other AHLs.**

**A)** Result of X-gal assay for checking auto-activation

of AHL proteins

[1 : DBD / AD, 2: DBD-GRAS / AD-Krev, 3: DBD-AHL1 / AD,

4: DBD-AHL2 / AD, 5: DBD-AHL5 / AD, 6: DBD-AHL6 / AD,

7: DBD-AHL7 / AD, 8: DBD-AHL8 / AD, 9: DBD-AHL10 / AD,

10: DBD-AHL12 / AD, 11: DBD-AHL13 / AD,

12: DBD-AHL15 / AD,13: DBD-AHL16 / AD,

14: DBD-AHL19 / AD, 15: DBD-AHL20 / AD,

16: DBD-AHL21 / AD, 17: DBD-AHL22 / AD,

18: DBD-AHL23 / AD,19: DBD-AHL27 / AD,

20: DBD-AHL29 / AD ]

**B)** Result of X-gal assay for checking between AHL

proteins and AHL4

[1 : DBD / AD, 2: DBD-GRAS / AD-Krev,

3: DBD-AHL1 / AD-AHL4, 4: DBD-AHL2 / AD-AHL4,

5: DBD-AHL3 / AD-AHL4, 6: DBD-AHL5 / AD-AHL4,

7: DBD-AHL6 / AD-AHL4, 8: DBD-AHL7 / AD-AHL4,

9: DBD-AHL8 / AD-AHL4, 10: DBD-AHL10 / AD-AHL4,

11: DBD-AHL12 / AD-AHL4, 12: DBD-AHL13 / AD-AHL4,

13: DBD-AHL15 / AD-AHL4, 14: DBD-AHL16 / AD-AHL4,

15: DBD-AHL17 / AD-AHL4, 16: DBD-AHL19 / AD-AHL4,

17: DBD-AHL20 / AD-AHL4, 18: DBD-AHL21 / AD-AHL4 ]

## AHL3 interacts with PPC domain of AHL4.

Neff's group reported that AHL27 protein and AHL29 protein interact with each other and this interaction is mediated by PPC domain (Zhao et al., 2013). Based on this information, we asked whether PPC domain of AHL4 is also critical for its interaction with AHL3 protein as well as other AHLs. We cloned the coding region of PPC domain in *AHL4* into pENTR/SD/D-TOPO vector using Invitrogen™ TOPO™ PCR Cloning and introduced it into the yeast expression vector by Invitrogen™ Gateway™ LR Clonase™ II enzyme mix with Gateway® Technology. Interaction between AHL3 and PPC domain of AHL4 protein was checked by X-gal assay (Figure 7). Native DBD and AD protein were used as negative control and DBD-Krev and AD-Gras protein were used as positive control. AHL3 auto-activation did not show. AHL3 with DBD interacts with PPC domain of AHL4 with AD.

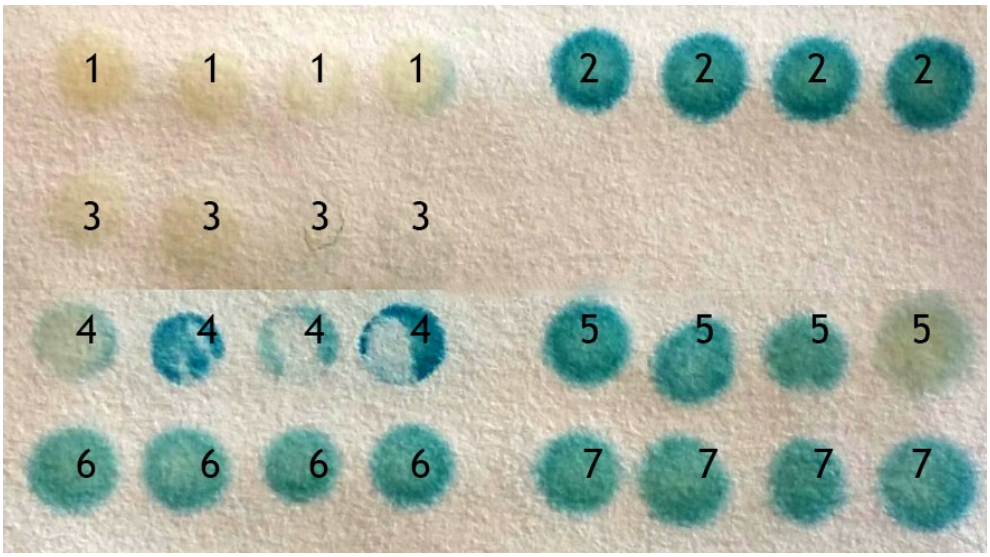


**Figure 7. Result of X-gal assay for checking between AHL3 and PPC domain of AHL4.**

[1 : DBD / AD , 2: DBD-GRAS / AD-Krev , 3: DBD-AHL3 / AD , 4: DBD-AHL3 / AD-AHL4 , 5: DBD- AHL3 / AD -PPC of AHL4 , 6: DBD-AHL3 / AD-AHL5 ,

7: DBD- AHL3 / AD-AHL12]

To investigate whether PPC domain of AHL4 protein can interact with other AHL proteins as it can with AHL3, we performed yeast-2-hybrid X-gal assay. When we checked auto-activation of PPC domain of AHL4 protein, we did not find auto-activation activity of PPC domain of AHL4. Therefore, we used PPC domain of AHL4 protein fused to DBD and analyzed its interaction with other AHL proteins that were fused to AD (Figure 8A). We also checked the interaction in reverse (Figure 8B, C). Interaction between AHL4-PPC domain fused to DBD and AHL proteins with AD was not detected. However, when we analyzed the interaction between AHL proteins with DBD and AHL4-PPC with AD, we found some AHL proteins can interact with PPC domain of AHL4 protein. Considering auto-activation of AHL proteins, AHL8 and AHL12 can interact with PPC domain of AHL4 protein.

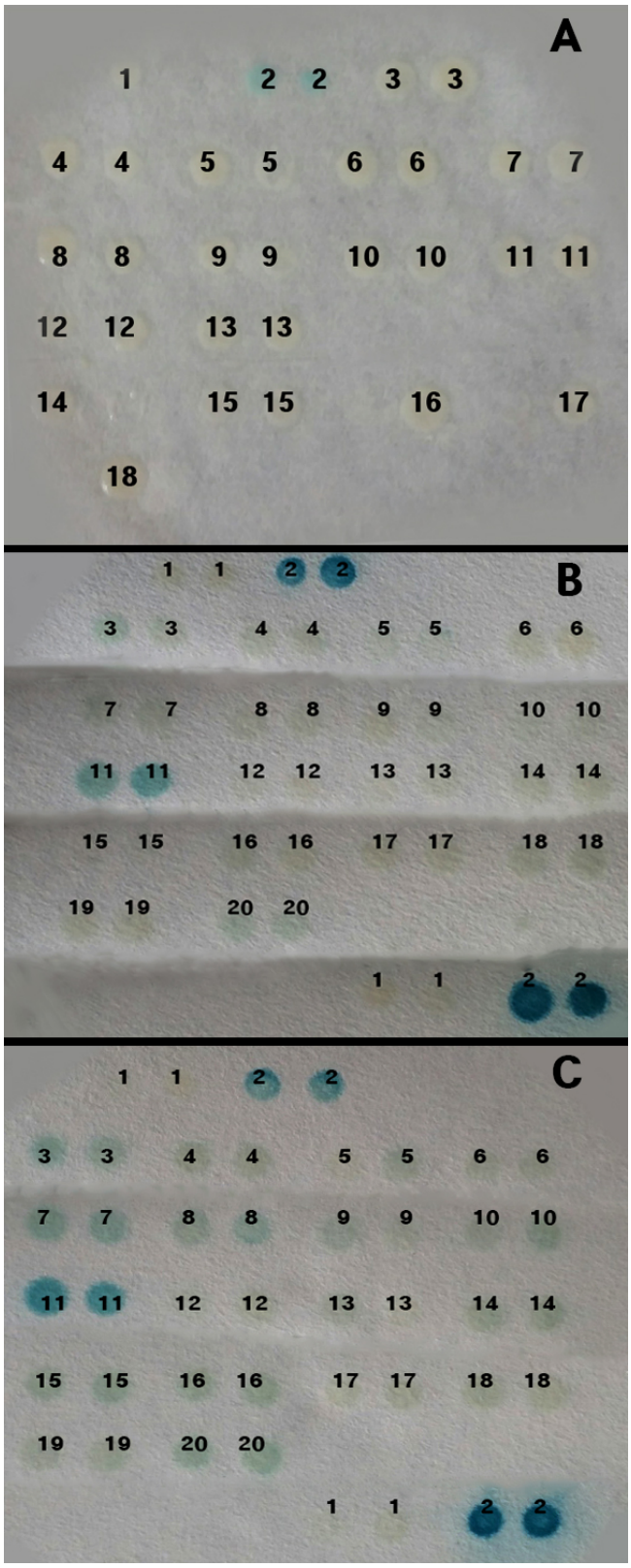
A
1 2 2 3 3
4 4 5 5 6 6 7 7
8 8 9 9 10 10 11 11
12 12 13 13
14 15 15 16 17
18
B
1 1 2 2
3 3 4 4 5 5 6 6
7 7 8 8 9 9 10 10
11 11 12 12 13 13 14 14
15 15 16 16 17 17 18 18
19 19 20 20
1 1 2 2
C
1 1 2 2
3 3 4 4 5 5 6 6
7 7 8 8 9 9 10 10
11 11 12 12 13 13 14 14
15 15 16 16 17 17 18 18
19 19 20 20
1 1 2 2

**Figure 8. Yeast-2-hybrid assay between PPC of AHL4 and other AHLs.**

**A)** Result of X-gal assay for checking between

PPC of AHL4 and other AHL

[1 : DBD / AD , 2: DBD-GRAS / AD-Krev ,

3: DBD-PPC of AHL4 / AD, 4: DBD-PPC of AHL4 / AD-AHL1,

5: DBD-PPC of AHL4/ AD-AHL2 6: DBD-PPC of AHL4/ AD-AHL3,

7: DBD-PPC of AHL4 / AD-AHL5, 8: DBD-PPC of AHL4 / AD-AHL6 9: DBD- PPC of AHL4 / AD-AHL7, 10: DBD- PPC of AHL4/ AD-AHL8,

11: DBD- PPC of AHL4 / AD-AHL10,

12: DBD- PPC of AHL4 / AD-AHL12,

13: DBD- PPC of AHL4 / AD-AHL13,

14: DBD- PPC of AHL4 / AD-AHL17,

15: DBD- PPC of AHL4 / AD-AHL20,

16: DBD- PPC of AHL4/ AD-AHL21,

17: DBD- PPC of AHL4/ AD-AHL23,

18: DBD- PPC of AHL4/ AD-AHL27]

**B)** Result of X-gal assay for checking auto-activation of AHL proteins

[1 : DBD / AD, 2: DBD-GRAS / AD-Krev, 3: DBD-AHL1 / AD,

4: DBD-AHL2 / AD, 5: DBD-AHL5 / AD, 6: DBD-AHL6 / AD,

7: DBD-AHL7 / AD, 8: DBD-AHL8 / AD, 9: DBD-AHL10 / AD,

10: DBD-AHL12 / AD, 11: DBD-AHL13 / AD,

12: DBD-AHL15 / AD, 13: DBD-AHL16 / AD,

14: DBD-AHL19 / AD, 15: DBD-AHL20 / AD,

16: DBD-AHL21 / AD, 17: DBD-AHL22 / AD,

18: DBD-AHL23 / AD, 19: DBD-AHL27 / AD,

20: DBD-AHL29 / AD ]

**C)** Result of X-gal assay for checking between AHL proteins and PPC of AHL4

[1 : DBD / AD, 2: DBD-GRAS / AD-Krev,

3: DBD-AHL1/AD- PPC of AHL4, 4: DBD-AHL2/AD-PPC of AHL4,

5: DBD-AHL5/AD-PPC of AHL4, 6: DBD-AHL6/AD-PPC of AHL4,

7: DBD-AHL7/AD-PPC of AHL4, 8: DBD-AHL8/AD-PPC of AHL4,

9: DBD-AHL10/AD-PPC of AHL4,

10: DBD-AHL12/AD-PPC of AHL4,

11: DBD-AHL13/AD-PPC of AHL4,

12: DBD-AHL15/AD-PPC of AHL4,

13: DBD-AHL16/AD-PPC of AHL4,

14: DBD-AHL19/AD-PPC of AHL4,

15: DBD-AHL20/AD-PPC of AHL4,

16: DBD-AHL21/AD-PPC of AHL4,

17: DBD-AHL22 / AD-PPC of AHL4,

18: DBD-AHL23 / AD-PPC of AHL4,

19: DBD-AHL27 / AD-PPC of AHL4,

20: DBD-AHL29 / AD-PPC of AHL4

## PPC domains of AHL proteins share a common 3D structure.

The 3D structure of PPC domain that seems important for protein-protein interaction has been resolved for a single PPC protein of prokaryote *Pyrococcus horikoshii* protein (*Ph*PPC) (Lin et al., 2007). The X-ray crystal structure suggests that this protein can form a trimer. The 3D structure of each PPC domain of AHLs in plant can be predicted based on the result from *Ph*PPC. The 3D structure of *Ph*PPC visualized using Pymol program shows anti-parallel β strands and one α helix (Figure 9A). Then, using SWISS program, the sequence of PPC domain of AHLs was aligned with the *Ph*PPC and the 3D structure was predicted (Arnold et al., 2006; Biasini et al., 2014; Guex et al., 2009; Kiefer et al., 2009) (figure 9B). In SWISS simulation, anti-parallel β strands in the PPC domain were contributing to protein-protein interaction. We chose AHL4 and AHL5 in clade B and choose AHL22 and AHL29 in clade A. Structure of every PPC domain of AHLs in clade A and clade B was predicted to be very similar to *Ph*PPC.

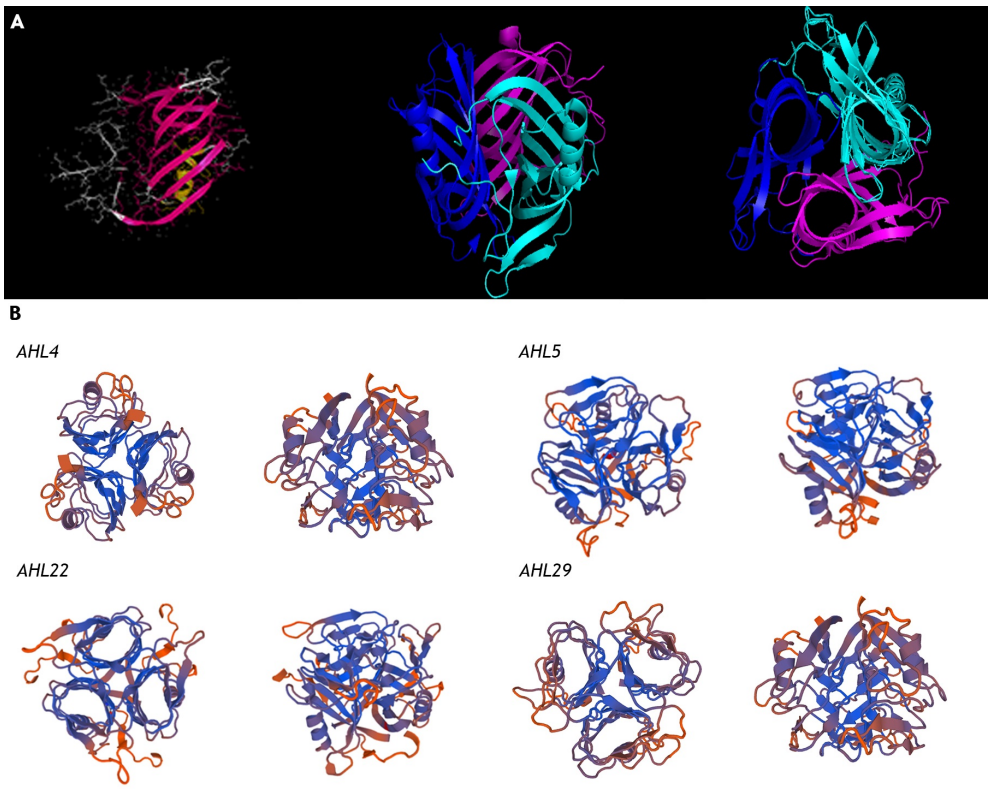


**Figure 9. *Ph*PPC and PPC domain of AHL proteins.**

A) 3D structure of *Ph*PPC. Yellow part is α helix structure and pink part is anti-parallel beta sheet. Gray part has no certain secondary structure in Pymol program.

B) 3D structures of PPC domain of AHLs. 4 of 29 AHLs were chosen as samples. AHL4 and AHL5 belongs to clade B. AHL22 and AHL29 belongs to clade A. Even though AHL proteins are located in different clades, they share a common 3D structure. Every AHL has one alpha helix and anti-parallel beta sheet structure like *Ph*PPC.

## Identification of amino-acids in PPC domain that are critical for protein-protein interaction.

Our investigation so far indicated that PPC domain is a major contributor to the protein-protein interaction. Studies of CPC and SHR protein found the presence of discrete amino acids that are responsible for protein-protein interaction or intercellular movement. These also suggested that protein-protein interaction significantly affects intercellular movement of CPC or SHR. Thus, we thought that there might be certain amino acids in PPC domain that are responsible for protein-protein interaction and that these amino acids might affect intercellular trafficking of AHL3 and 4.

Our examination of 3D structure of PPC domain in *Ph*PPC and AHL proteins indicated that PPC domain structure is well conserved (Figure 9). We also found few amino acid sequences that are highly conserved. Considering into conserved structure and amino acids between *Ph*PPC and AHL proteins, we chose three amino acids as candidates. These amino acids were determined in consultation with Professor Hee-Jung Choi. Based on this prediction, we mutated three amino acids in PPC domain of AHL4 proteins to Alanine (Figure 10) and then checked the interaction between the mutated AHL4 and other AHL proteins using yeast-2-hybrid assay. The location of each amino acid in 3D structure is indicated in Figure 10A. The alignment of PPC sequences and locations of mutate amino acids in sequences are indicated in Figure 10B. Yeast-2-hybrid assay between mutated

AHL4 protein (AHL4*) and AHL3 indicated that AHL4* does not interact with AHL3 protein (Figure 5A).

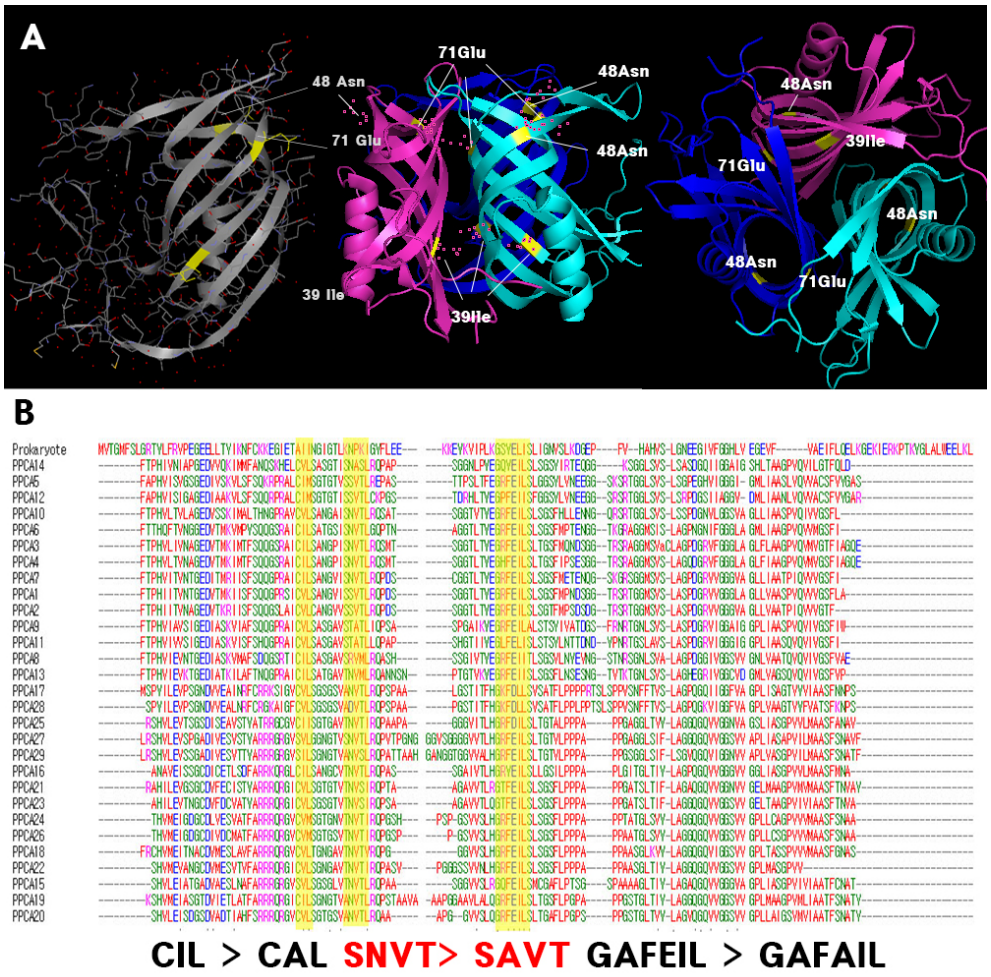


**Figure 10. Three amino acids that were selected for site-directed mutagenesis.**

A) Positions of selected three amino acids in 3D structure of *Ph*PPC. 39Ile, 48Asn and 71Glu are selected. 39Ile and 71Glu are located in the surface of interaction when PPC proteins make trimmer, while 48Asn is located in opposite site of the surface of interaction.

B) Positions of three amino acids which are planned to mutated. Aligned amino-acids of PPC domain show highly conserved sequences.

## Protein-protein interaction of AHL4 affects its intercellular movement.

According to the result of x-gal assay with mutated AHL4, amino acid sequence of PPC domain is important for AHL4 interact with other AHL proteins including AHL3. To investigate whether protein-protein interaction mediated by PPC domain affects intercellular movement of AHL4, we designed to generate a synthetic protein, $AHL4^{PPC\text{-}AHL5}$, in which PPC domain of AHL4 was replaced with PPC domain of AHL5 protein.

Because when we did yeast-2-hybrid assay between AHL3 and $AHL4^{PPC\text{-}AHL5}$, there was no interaction between two proteins (Figure 11A). We decided to make a GFP fusion line for investigating the movement of $AHL4^{PPC\text{-}AHL5}$.

$AHL4^{PPC\text{-}AHL5}$ translationally fused to GFP was expressed under AHL4 promoter in *ahl4-1* mutant. When we analyzed the $AHL4^{PPC\text{-}AHL5}$-GFP under confocal microscope, we found GFP signals in the root cap, columella, stele, endodermis, cortex and epidermis (Figure 11C). On the other hands, the AHL4-GFP expressed under the same AHL4 promoter was detected in the endodermis and stele. The GFP intensity of $AHL4^{PPC\text{-}AHL5}$-GFP was also higher than the intensity of AHL4-GFP (Figure 11B).

To find where AHL4 gene is transcribed, AHL4::GUS transgenic plant in the wild

type was examined again The GUS signal in 5 day old seedling roots was detected in the stele procambium and slightly in the root cap cells (Figure 11D).

These data suggest that AHL4$^{PPC\text{-}AHL5}$-GFP protein might move more actively than AHL4-GFP. Therefore, we conclude that protein-protein interaction mediated by PPC domain affects intercellular cell-to-cell movement of AHL4.

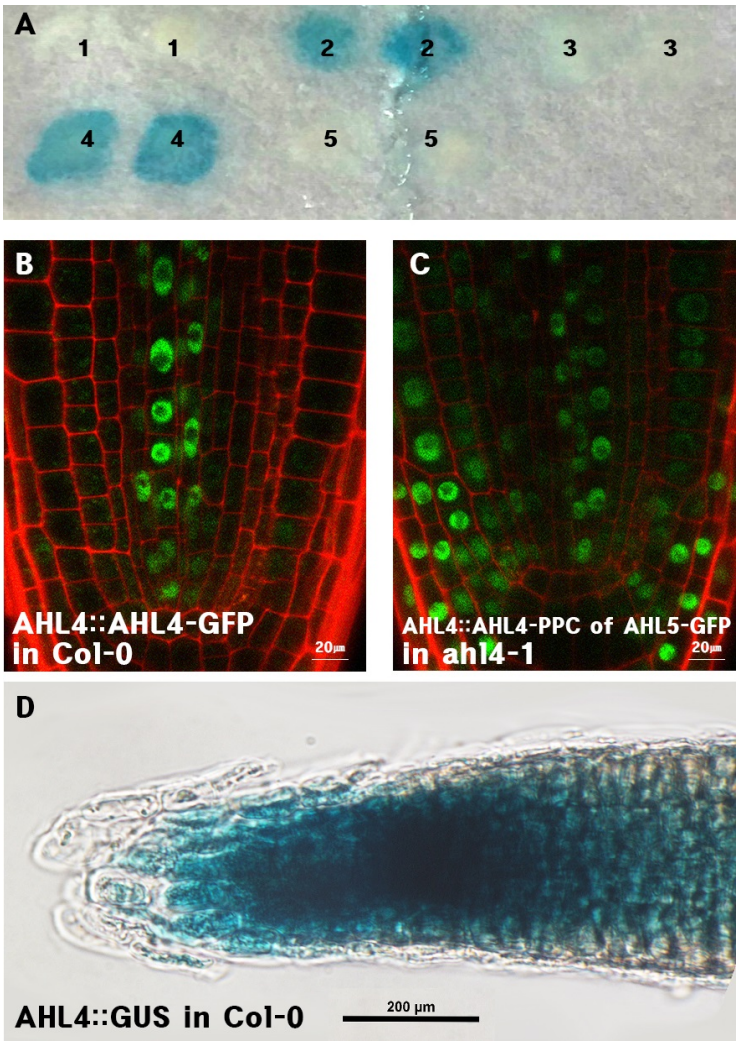


**Figure 11. Yeast-2-hybrid assay with - $AHL4^{PPC\text{-}AHL5}$/ Translational expression pattern of AHL4 and - $AHL4^{PPC\text{-}AHL5}$/ Transcriptional expression pattern of AHL4.**

A) Yeast-2-hybrid assay between AHL3 and other AHLs

[1 : DBD / AD , 2: DBD-GRAS / AD-Krev , 3: DBD-AHL3 / AD ,

4: DBD-AHL3 / AD-AHL4 , 5: DBD- AHL3 / AD- $AHL4^{PPC\text{-}AHL5}$

B) GFP expression of AHL4 translational fusion line. X400 White scale bar = 20㎛

C) GFP expression of AHL4-PPC of AHL5 translational fusion line X400

D) GUS expression of AHL4::GUS line X100 Black scale bar = 200㎛

# Ⅳ. Discussion

## AHL3 and AHL4 can make a protein complex with diverse AHLs.

Based on extensive yeast-2-hybrid experiments using AHL3 and AHL4 as baits, we inferred the interaction map of AHL3 and AHL4 (Figure 12). AHL3 and AHL4 interact with other AHLs which are expressed in root stele and their interaction overlaps partially. The fact that AHL3 and AHL4 can interact with other AHLs suggests that AHL3/4 can generate diverse forms of protein complexes by interacting with various AHL members.

The members of clade B which AHL3 and AHL4 belong to has a trend to interact with AHL3 and AHL4. Only AHL8 did not interact with either AHL3 or AHL4. On the other hands, only one member of clade A interacts with AHL3 and AHL4. AHL15 can interact with AHL3 and AHL4. The critical difference between clade A and clade B is the sequence of PPC domain (Figure 3). Therefore, the type of PPC domain might be a major factor that decides protein-protein interaction.

AHLs which interact with both AHL3 and AHL4 are AHL1, AHL6, AHL7, AHL10 and AHL12. These AHLs can make protein complex with AHL3/AHL4. Especially, expression level of AHL1 is higher than the level of AHL3 and AHL4

in the root stele (Figure 4). Therefore, we can focus on AHL1 protein for investigating how AHLs form hetero-complexes.

## The difference between mutated amino acids of PPC domain of AHL4.

As in the case of AHL27 and AHL29 (Zhao et al., 2013), the PPC domain seems to be important for the interaction between AHL3 and AHL4. The fact that interaction trend between AHLs of clade A and AHLs of clade B is different also supports the thought that sequence of PPC domain is important for determining protein-protein interaction among AHL members. The X-gal assay result of AHL4* suggests that certain amino acids might be critical for interaction between AHL proteins (Figure 5).

The interaction data suggest the possibility that AHL3 and AHL4 make not only a trimer but also a larger complex beyond trimers. The selected three amino acids have some different properities. $Ile^{39}$ and $Glu^{71}$ are located on the surface of interaction when *Ph*PPC makes a trimer, while $Asn^{48}$ is located in opposite site of the surface of interaction (Figure 9). Therefore, $Ile^{39}$ and $Glu^{71}$ might be important to make a trimer and $Asn^{48}$ might be important to make a larger complex. We are planning to make mutations only on $Ile^{39}$ and $Glu^{71}$ and check interaction ability.

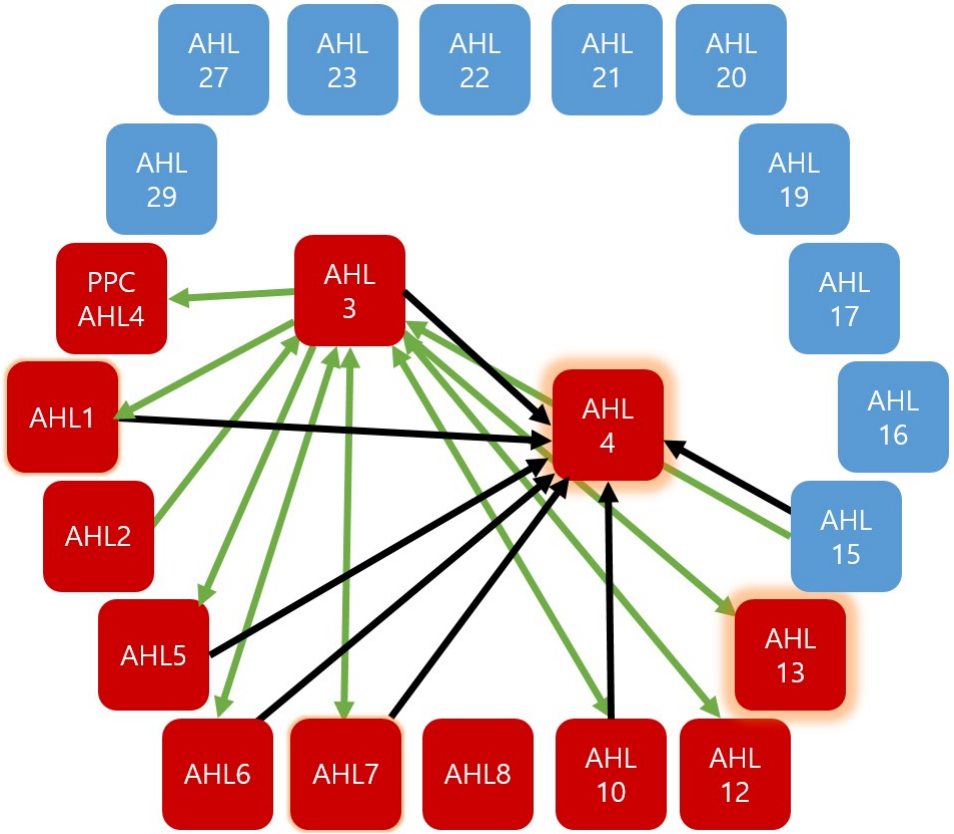


**Figure 12. The interaction map of AHL3 and AHL4.**

Red box is AHLs belonged to clade B. Blue box is AHLs belonged to clade A. Glow indicates auto-activation. Each arrows direct from bait to prey. Green arrows indicate interaction with AHL3. Black arrows indicate interaction with AHL4. All data is confirmed by X-gal assay.

## The relationship between interaction and movement of AHL4.

There are two hypothesis about the relationship between protein-protein interaction and intercellular movement of AHL4 protein. The first one is there is a critical amino-acids which participates in both interaction and movement. In case of the first hypothesis, interaction and movement can disrupt together when we induce to mutate certain amino acids. The result of swapping of PPC domain between AHL4 and AHL5 assists that interaction can effect on movement.

Another hypothesis is there are two inter-dependent parts which participate in interaction and movement of AHL4, respectively.

The case of AHL1 protein can assist the latter hypothesis. AHL1 and AHL4 have similar characters. They are highly expressed in the root stele and both proteins are belong to clade B. Both proteins can interact with AHL3. However, In case of AHL1, the protein does not move into endodermis cell from stele, while AHL4 proteins can move (Figure 13)

When we aligned with AHL1 and AHL4 sequences, Aligned amino-acids of PPC domain show highly conserved sequences. However, the remained sequence is different. This facts suggest another possibility that there is another critical amino-acids which is independent of interaction and located outside the PPC domain.

To clarify the hypothesis, we will try to make various fusion proteins of AHL4 and AHL1 and classify fusion proteins into two group: moved protein and no-moved protein. Using this approach, we might be able to address the relationships between protein-protein interaction and intercellular protein trafficking in more detail.

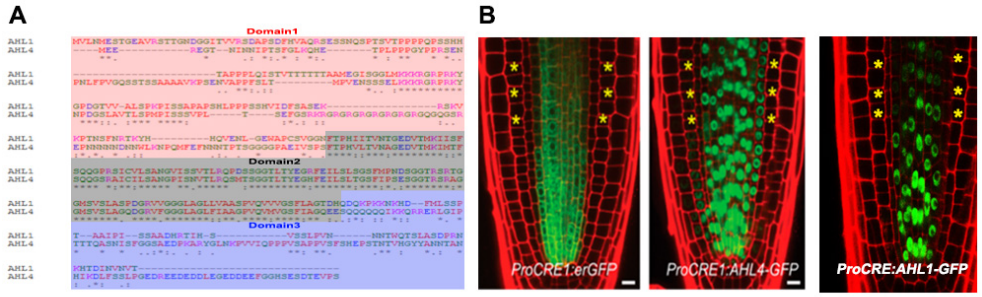


**Figure 13. Sequence alignment and movement of AHL1 and AHL4.**

A) AHL1 and AHL4 have a conserved sequence of PPC domain (domain 2), while the remained sequences (domain 1 and domain 3) is highly different.

B)AHL4 protein can move into endodermis cell compared to its transcriptional fusion. AHL1 protein cannot move into endodermis cell. White scale bar = 10$\mu$m

# Ⅴ. References

Aravind, L., and Landsman, D. (1998). AT-hook motifs identified in a wide variety of DNA-binding proteins. Nucleic Acids Res *26*, 4413–4421.

Arnold, K., Bordoli, L., Kopp, J., and Schwede, T. (2006). The SWISS-MODEL workspace: a web-based environment for protein structure homology modelling. Bioinformatics *22*, 195-201.

Benfey, P.N., Linstead, P.J., Roberts, K., Schiefelbein, J.W., Hauser, M.-T., and Aeschbacher, R.A. (1993). Root development in Arabidopsis: four mutants with dramatically altered root morphogenesis. Development *119*, 57-70.

Bernhardt, C., Lee, M.M., Gonzalez, A., Zhang, F., Lloyd, A., and Schiefelbein, J. (2003). The bHLH genes GLABRA3 (GL3) and ENHANCER OF GLABRA3 (EGL3) specify epidermal cell fate in the Arabidopsis root. Development *130*, 6431-6439.

Bernhardt, C., Zhao, M., Gonzalez, A., Lloyd, A., and Schiefelbein, J. (2005). The bHLH genes GL3 and EGL3 participate in an intercellular regulatory circuit that controls cell patterning in the Arabidopsis root epidermis. Development *132*, 291-298.

Biasini, M., Bienert, S., Waterhouse, A., Arnold, K., Studer, G., Schmidt, T., Kiefer, F., Gallo Cassarino, T., Bertoni, M., Bordoli, L.*, et al.* (2014). SWISS-MODEL: modelling protein tertiary and quaternary structure using evolutionary information. Nucleic Acids Res *42*, W252-258.

Bishopp, A., Help, H., El-Showk, S., Weijers, D., Scheres, B., Friml, J., Benkova, E., Mahonen, A.P., and Helariutta, Y. (2011). A Mutually Inhibitory Interaction

between Auxin and Cytokinin Specifies Vascular Pattern in Roots. Curr Bio *21*, 917-926.

Brady, S.M., Orlando, D.A., Lee, J.-Y., Wang, J.Y., Koch, J., Dinneny, J.R., Mace, D., Ohler, U., and Benfey, P.N. (2007). A High-Resolution Root Spatiotemporal Map Reveals Dominant Expression Patterns. Science *318*, 801-806.

Carlsbecker, A., Lee, J.-Y., Roberts, C.J., Dettmer, J., Lehesranta, S., Zhou, J., OveLindgren, Moreno-Risueno, M.A., AnneVate, J.L.B., Helariutta, Y.*, et al.* (2010). Cell signalling by microRNA165/6 directs gene dose-dependent root cell fate. Nature *465*, 316-321.

Clough, S.J., and Bent, A.F. (1998). Floral dip: a simplified method for Agrobacterium-mediated transformation of Arabidopsis thaliana. Plant J *16*, 735-743.

Crawford, K.M., and Zambryski, P.C. (2000). Subcellular localization determines the availability of non-targeted proteins to plasmodesmatal transport. Curr Bio *10*, 1032–1040.

Crawford, K.M., and Zambryski, P.C. (2001). Non-Targeted and Targeted Protein Movement through Plasmodesmata in Leaves in Different Developmental and Physiological States. Plant Physiol *125*, 1802-1812.

Cristina, M.D., Sessa, G., Dolan, L., Linstead, P., Baima, S., Ruberti, I., and Morelli, G. (1996). The Arabidopsis Athb-10 (GLABRA2) is an HD-Zip protein required for regulation of root hair development. Plant J *10*, 393-402.

Cui, H., Levesque, M.P., Vernoux, T., Jung, J.W., Paquette, A.J., Gallagher, K.L., Wang, J.Y., Blilou, I., Scheres, B., and Benfey, P.N. (2007). An Evolutionarily Conserved Mechanism Delimiting SHR Movement Defines a Single Layer of

Endodermis in Plants. Science *316*, 421-425.

De Rybel, B., Moller, B., Yoshida, S., Grabowicz, I., Barbier de Reuille, P., Boeren, S., Smith, R.S., Borst, J.W., and Weijers, D. (2013). A bHLH complex controls embryonic vascular tissue establishment and indeterminate growth in Arabidopsis. Dev Cell *24*, 426-437.

Dolan, L., Duckett, C.M., Grierson, C., Linstead, P., Schneider, K., Lawson, E., Dean, C., Poethig, S., and Roberts, K. (1994). Clonal relationships and cell patterning in the root epidermis of Arabidopsis. Development *120*, 2465-2474.

Dolan, L., Janmaat, K., Willemsen, V., Linstead, P., Poethig, S., Roberts, K., and Scheres, B. (1993). Cellular organisation of the Arabidopsis thaliana root. Development *119*, 71-84.

Emery, J.F., Floyd, S.K., Alvarez, J., Eshed, Y., Hawker, N.P., Izhaki, A., Baum, S.F., and Bowman, J.L. (2003). Radial patterning of Arabidopsis shoots by class III HD-ZIP and KANADI genes. Curr Bio *13*, 1768-1774.

Etchells, J.P., and Turner, S.R. (2010). The PXY-CLE41 receptor ligand pair defines a multifunctional pathway that controls the rate and orientation of vascular cell division. Development *137*, 767-774.

Fisher, K., and Turner, S. (2007). PXY, a receptor-like kinase essential for maintaining polarity during plant vascular-tissue development. Current biology : CB *17*, 1061-1066.

Fujimoto, S., Matsunaga, S., Yonemura, M., Uchiyama, S., Azuma, T., and Fukui, K. (2004). Identification of a novel plant MAR DNA binding protein localized on chromosomal surfaces. Plant Mol Biol *56*, 225-239.

Gallagher, K.L., Paquette, A.J., Nakajima, K., and Benfey, P.N. (2004).

Mechanisms Regulating SHORT-ROOT Intercellular Movement. Curr Bio *14*, 1847-1851.

Galway, M.E., Masucci, J.D., Lloyd, A.M., Walbot, V., Davis, R.W., and Schiefelbein, J.W. (1994). The TTG Gene Is Required to Specify Epidermal Cell Fate and Cell Patterning in the Arabidopsis Root. Dev Biol *166*, 740-754.

Guex, N., Peitsch, M.C., and Schwede, T. (2009). Automated comparative protein structure modeling with SWISS-MODEL and Swiss-PdbViewer: a historical perspective. Electrophoresis *30 Suppl 1*, S162-173.

Helariutta, Y., Fukaki, H., Wysocka-Diller, J., Nakajima, K., Jung, J., Sena, G., Hauser, M.-T., and Benfey, P.N. (2000). The SHORT-ROOT gene controls radial patterning of the Arabidopsis root through radial signaling. Cell *101*, 555–567.

Hung, C.-Y., Lin, Y., Zhang, M., Pollock, S., Marks, M.D., and Schiefelbein, J. (1998). A Common Position-Dependent Mechanism Controls Cell-Type Patterning and GLABRA2 Regulation in the Root and Hypocotyl Epidermis of Arabidopsis. Plant Physiol *117*, 73-84.

Huth, J.R., Bewley, C.A., Nissen, M.S., Evans, J.N.S., Reeves, R., Gronenborn, A.M., and Clore, G.M. (1997). The solution structure of an HMG-I(Y)–DNA complex defines a new architectural minor groove binding motif. Nat Struct Biol *4*, 657-665.

Kiefer, F., Arnold, K., Kunzli, M., Bordoli, L., and Schwede, T. (2009). The SWISS-MODEL Repository and associated resources. Nucleic Acids Res *37*, D387-392.

Koshino-Kimura, Y., Wada, T., Tachibana, T., Tsugeki, R., Ishiguro, S., and Okada, K. (2005). Regulation of CAPRICE transcription by MYB proteins for root

epidermis differentiation in Arabidopsis. Plant Cell Physiol *46*, 817-826.

Kurata, T., Ishida, T., Kawabata-Awai, C., Noguchi, M., Hattori, S., Sano, R., Nagasaka, R., Tominaga, R., Koshino-Kimura, Y., Kato, T.*, et al.* (2005). Cell-to-cell movement of the CAPRICE protein in Arabidopsis root epidermal cell differentiation. Development *132*, 5387-5398.

Laurenzio, L.D., Wysocka-Diller, J., Malamy, J.E., Pysh, L., Helariutta, Y., Freshour, G., Hahn, M.G., Feldmann, K.A., and Benfey, P.N. (1996). The SCARECROW gene regulates an asymmetric cell division that is essential for generating the radial organization of the Arabidopsis root. Cell *86*, 423-433.

Lee, J.Y., Colinas, J., Wang, J.Y., Mace, D., Ohler, U., and Benfey, P.N. (2006). Transcriptional and posttranscriptional regulation of transcription factor expression in Arabidopsis roots. Proc Natl Acad Sci U S A *103*, 6055-6060.

Lee, M.M., and Schiefelbein, J. (1999). WEREWOLF, a MYB-Related Protein in Arabidopsis, Is a Position-Dependent Regulator of Epidermal Cell Patterning. Cell *99*, 473–483.

Lin, L., Nakano, H., Nakamura, S., Uchiyama, S., Fujimoto, S., Matsunaga, S., Kobayashi, Y., Ohkubo, T., and Fukui, K. (2007). Crystal structure of Pyrococcus horikoshii PPC protein at 1.60 Å resolution. Proteins: Structure, Function, and Bioinformatics *67*, 505-507.

Lin, L., Nakano, H., Uchiyama, S., Fujimoto, S., Matsunaga, S., Nakamura, S., Kobayashi, Y., Ohkubob, T., and Fukuia, K. (2005). Crystallization and preliminary X-ray crystallographic analysis of a conserved domain in plants and prokaryotes from Pyrococcus horikoshii OT3. Acta Cryst *61*, 414-416.

Mahonen, A.P., Bishopp, A., Higuchi, M., Nieminen, K.M., Kinoshita, K.,

Tormakangas, K., Ikeda, Y., Oka, A., Kakimoto, T., and Helariutta, Y. (2006). Cytokinin signaling and its inhibitor AHP6 regulate cell fate during vascular development. Science *311*, 94-98.

Matsubayashi, Y., Yang, H., and Sakagami, Y. (2001). Peptide signals and their receptors in higher plants. TRENDS in Plant Science *6*, 573-577.

Morohashi, K., Minami, M., Takase, H., Hotta, Y., and Hiratsuka, K. (2003). Isolation and characterization of a novel GRAS gene that regulates meiosis-associated gene expression. The Journal of biological chemistry *278*, 20865-20873.

Oparka, K.J., Roberts, A.G., Boevink, P., Cruz, S.S., Roberts, I., Pradel, K.S., Imlau, A., Kotlizky, G., Sauer, N., and Epel, B. (1999). Simple, but Not Branched, Plasmodesmata Allow the Nonspecific Trafficking of Proteins in Developing Tobacco Leaves. Cell *97*, 743–754.

Rerie, W.G., Feldmann, K.A., and Marks, M.D. (1994). The GLABRA2 gene encodes a homeo domain protein required for normal tnchome development in Arabidopsis. Genes Dev *8*, 1388-1399.

Sabatini, S., Heidstra, R., Wildwater, M., and Scheres, B. (2003). SCARECROW is involved in positioning the stem cell niche in the Arabidopsis root meristem. Genes Dev *17*, 354-358.

Schlereth, A., Moller, B., Liu, W., Kientz, M., Flipse, J., Rademacher, E.H., Schmid, M., Jurgens, G., and Weijers, D. (2010). MONOPTEROS controls embryonic root initiation by regulating a mobile transcription factor. Nature *464*, 913-916.

Sena, G., Jung, J.W., and Benfey, P.N. (2004). A broad competence to respond to SHORT ROOT revealed by tissue-specific ectopic expression. Development *131*, 2817-2826.

Serebriiskii, I., Khazak, V., and Golemis, E.A. (1999). A Two-hybrid Dual Bait System to Discriminate Specificity of Protein Interactions. J Biol Chem *274*, 17080-17087.

Simon, M., Lee, M.M., Lin, Y., Gish, L., and Schiefelbein, J. (2007). Distinct and overlapping roles of single-repeat MYB genes in root epidermal patterning. Dev Biol *311*, 566-578.

Sozzani, R., Cui, H., Moreno-Risueno, M.A., Busch, W., Van Norman, J.M., Vernoux, T., Brady, S.M., Dewitte, W., Murray, J.A., and Benfey, P.N. (2010). Spatiotemporal regulation of cell-cycle genes by SHORTROOT links patterning and growth. Nature *466*, 128-132.

Street, I.H., Shah, P.K., Smith, A.M., Avery, N., and Neff, M.M. (2008). The AT-hook-containing proteins SOB3/AHL29 and ESC/AHL27 are negative modulators of hypocotyl growth in Arabidopsis. The Plant journal : for cell and molecular biology *54*, 1-14.

Tominaga-Wada, R., Nukumizu, Y., Sato, S., and Wada, T. (2013). Control of Plant Trichome and Root-Hair Development by a Tomato (Solanum lycopesicum) R3 MYB Transcription Factor. PLos One *8*, e54019.

Wada, T., Kurata, T., Tominaga, R., Koshino-Kimura, Y., Tachibana, T., Goto, K., Marks, M.D., Shimura, Y., and Okada, K. (2002). Role of a positive regulator of root hair development, CAPRICE, in Arabidopsis root epidermal cell differentiation. Development *129*, 5409-5419.

Wada, T., Tachibana, T., Shimura, Y., and Okada, K. (1997). Epidermal Cell Differentiation in Arabidopsis Determined by a Myb Homolog, CPC. Science *277*, 1113-1116.

Walker, A.R., Davison, P.A., Bolognesi-Winfield, A.C., James, C.M., Srinivasan, N., Blundell, T.L., Esch, J.J., Marks, M.D., and Gray, J.C. (1999). The TRANSPARENT TESTA GLABRA1 Locus, Which Regulates Trichome Differentiation and Anthocyanin Biosynthesis in Arabidopsis, Encodes a WD40 Repeat Protein. Plant Cell, 1337–1349.

Xiao, C., Chen, F., Yu, X., Lin, C., and Fu, Y.-F. (2009). Over-expression of an AT-hook gene, AHL22, delays flowering and inhibits the elongation of the hypocotyl in Arabidopsis thaliana. Plant Mol Biol *71*, 39-50.

Zambryski, P., and Crawford, K. (2000). PLASMODESMATA: Gatekeepers for Cell-to-Cell Transport ofDevelopmental Signals in Plants. AnnuRevCellDevBiol *16*, 393–421.

Zhao, J., Favero, D.S., Peng, H., and Neff, M.M. (2013). Arabidopsis thaliana AHL family modulates hypocotyl growth redundantly by interacting with each other via the PPC/DUF296 domain. Proc Natl Acad Sci U S A, 4688-4697.

Zhou, G.K., Kubo, M., Zhong, R., Demura, T., and Ye, Z.H. (2007). Overexpression of miR165 affects apical meristem formation, organ polarity establishment and vascular development in Arabidopsis. Plant Cell Physiol *48*, 391-404.

Zhou, J., Wang, X., Lee, J.-Y., and Lee, J.-Y. (2013). Cell-to-Cell Movement of Two Interacting AT-Hook Factors in Arabidopsis Root Vascular Tissue Patterning. Plant Cell *25*, 187-201.

# 국문초록

# AT-HOOK MOTIF NUCLEAR LOCALIZED PROTEIN 3 (AHL3) / AHL4 전사인자 사이의 상호작용과 세포 간 이동 연구

다양한 단백질 사이의 상호작용과 세포간 단백질 이동은 세포의 운명 결정에 있어서 필수적인 과정이다. 최근, 두 개의 새로운 AT-HOOK MOTIF NUCLEAR LOCALIZED PROTEIN 3 (AHL3) 와 AHL4 단백질이 애기 장대 뿌리의 분화에서 물관의 경계를 설정하는데 관여한다는 점이 알려졌다. 이 두 인자들은 서로 상호작용을 보이며, 이웃한 세포로 이동하는 성격을 가지고 있다. 그러나 어떠한 도메인이 이들의 상호작용과 세포간 이동에 관여하는지는 알려지지 않았다.

AHL 단백질 패밀리 구성원들은 AT-hook motif 와 plant and prokaryote conserved (PPC) domain의 두 개의 보존된 도메인들을 가지고 있다. 본 연구에서는 AHL4의 PPC 도메인이 AHL3을 포함한 다른 AHL들과 AHL4가 상호작용하는데 있어서 관여하는 것을 발견하였

다. PPC 도메인의 아미노산 서열의 중요성을 이해하기 위래, 3D 구조상 단백질 사이의 상호작용에 관여할 것이라 생각되는 AHL4 단백질의 PPC 도메인에 위치한 몇 개의 아미노산을 돌연변이 시켰다. 효모-2-혼성화 실험은 돌연변이 시킨 AHL4 단백질과 AHL3 단백질이 더 이상 상호작용하지 않는 것을 보여주었다. 또한 AHL3과 AHL4 사이는 그들 뿐 아니라 다른 AHL들과도 상호작용을 보인다. 이러한 단백질 상호작용 자료는  AHL 단백질 사이의 단백질 복합체가 형성되는데 PPC 도메인의 특정 아미노산이 중요할 것임을 알려준다. 또한 PPC 도메인을 AHL사이에서 바꾸게 되면 AHL의 이동이 변화하는 것을 확인하였다. 따라서 PPC 도메인에 의한 단백질 간 상호작용이 AHL의 이동에도 관여할 것이라 생각된다.

**주요어: 단백질 사이의 상호작용, 세포간 이동, AT-HOOK MOTIF NUCLEAR LOCALIZED PROTEIN (AHL) , plant and prokaryote conserved (PPC) domain**

Student Number: 2014-25017